TORSIONAL NATURAL FREQUENCIES:
MEASUREMENT VS. PREDICTION

Qingyu Wang
Mechanical Engineer
Elliott Group
Jeannette, Pennsylvania

Troy D. Feese
Senior Staff Engineer
Engineering Dynamics Inc.
San Antonio, Texas

Brian C. Pettinato
Manager, Product Development
Elliott Group
Jeannette, Pennsylvania

Qingyu Wang is a Mechanical Engineer at Elliott Group in Jeannette, Pennsylvania. He has been with Elliott Group since 2005. His areas of expertise include lateral and torsional rotordynamics. He received his B.S. and M.S. both in Mechanical Engineering from Tsinghua University, 1997 and 2000 respectively. He received his Ph.D in Mechanical Engineering from the University of Virginia, 2008. He serves on the API 684 rotordynamics task force, and is a member of ASME.

Troy Feese is a Senior Staff Engineer at Engineering Dynamics Incorporated (EDI) in San Antonio, Texas. He has 22 years of experience performing torsional vibration, lateral critical speed, and rotordynamic stability analyses as well as evaluating structures using finite element methods. He conducts field studies of rotating machinery, reciprocating equipment, piping, structures, and foundations. He is a lecturer at the annual EDI seminar and has published technical papers on torsional vibration, lateral critical speeds, and balancing. He received a BSME from The University of Texas at Austin and has a MSME from UTSA. He is a member of ASME, Vibration Institute, contributed to API 684, was a speaker at NPRA, and is a licensed Professional Engineer in Texas.

Brian C. Pettinato is Manager of Product Development at Elliott Group in Jeannette, Pennsylvania. He has been with Elliott Group since 1995. His areas of expertise include lateral and torsional rotordynamics, vibration analysis, and the testing and evaluation of fluid film journal bearings. He currently manages a group

responsible for compressor and expander technology development. Prior to joining Elliott Group, Mr. Pettinato worked as a project engineer for an aftermarket bearing manufacturer. Mr. Pettinato received his B.S. (Mechanical Engineering, 1989) and M.S. (Mechanical Engineering, 1992) degrees from the University of Virginia. He has coauthored over ten technical papers, and holds one U.S. patent. He is a registered Professional Engineer in the State of Pennsylvania. He serves on the API 684 rotordynamics task force, and is a member of both ASME and STLE.

ABSTRACT

Excessive torsional vibration can cause damage or failure to rotating equipment trains thereby resulting in costly shutdowns. A comprehensive torsional vibration analysis is the typical method of designing a torsional system that avoids such problems.

Requirements of a torsional system design are commonly based on the API Standards (API 617, 2002 and API 684, 2005). These standards require torsional natural frequencies (TNFs) to have at least 10% separation margin (SM) from any excitation frequency. If the recommended SM cannot be achieved, then the torsional system design must be shown to be acceptable by stress analysis. The validity of the predicted TNF and any stress analysis is dependent on the accuracy of the model.

Some degree of uncertainty is always present within the analytical data, the modeling techniques, and the assumptions for excitation and damping. This paper provides an uncertainty study of more than ten (10) torsional systems. Major sources of uncertainty in torsional modeling are identified. The effect of variation in mass-elastic data is examined, and a comparison between measured and predicted TNFs for numerous cases is presented. Based on the studies and measurements, a reasonable SM range is presented, and 5% SM for measured TNFs is proposed.

INTRODUCTION

The design of safe and reliable turbomachinery requires proper vibration isolation by considering the lateral and torsional rotordynamics. Torsional vibration is the focus of this paper.

API standards have required a torsional analysis since 1973 (API 617, 1973). These torsional requirements have evolved over time such as discussed by Pettinato, et al., 2011. The primary requirement of the API standard is a separation margin of 10% from excitation frequencies, especially running speeds, 2× running speeds, and one and two times electrical line frequency when applicable. The method of achieving acceptable torsional separation margin is generally limited to coupling selection and tuning, and in some cases modification of system inertia. There are limits to how far a torsional natural frequency can be shifted, and the required 10% SM cannot always be achieved, and the API standard allows for torsional system justification by stress analysis in these situations. Unavoidable violation of 10% SM requirement is not uncommon for certain systems, such as variable speed systems with large operating speed range or reciprocating systems with closely spaced excitation frequencies. It is assumed that these API recommendations refer to calculated results performed in the design stage. (Other criteria related to synchronous motor startup analysis and transient events such as electrical faults are not within the scope of this paper.)

Unlike lateral critical speeds, torsional critical speeds do not require verification. Consequently, torsional system accuracy has not been benchmarked on a massive scale. Whereas torsional measurement during complete string test has been an option within API 617 since 1988, it has rarely been selected by end users. This is due in part to the expense and difficulty of a full string test.

Despite the lack of benchmarking, there are relatively few torsional failures related to insufficient separation margin from running speed. For example, Elliott Group has over 40 units in operation with insufficient margin from 2× compressor running speed, all justified by stress analysis, and all having no problems. Insufficient margin from 1× running speed could be of greater concern especially for certain torsional mode shapes. High risk cases that can be improved by separation margin include avoidance of pressure pulsation excitation (Feese and Hill, 2009), and avoidance of transient startup and fault excitation due to 1× and 2× line frequency (Vance et al., 1984) such as occurs due to motor or generator applications, each of which can be improved by having good separation margin from these excitation frequencies, which are non-synchronous.

A torsional analysis that is performed utilizing good modeling techniques, a proven computer program, and accurate mass-elastic data is generally considered to have accuracy for the primary TNFs of ±5%. There have been only a few comparisons made between predictions and measurements.

LITERATURE REVIEW

Lateral Natural Frequency Accuracy

Lateral critical speed predictions are required by API standards to be within ±5% of the measured values. Lateral systems include significant damping, and complicated hydrodynamic effects, and would therefore seem to be more difficult to predict than a torsional system. In the case of lateral dynamics of rotor-bearing systems, Vance, et al., (1984) investigated rotor natural frequencies in both the free-free state and the fluid film bearing supported state. Major sources of error were attributed to modeling the fits of shrunk-on components. The prediction error of turbomachinery lateral natural frequencies was cited as being within 7% for rotors when considering bearing and foundation properties as well as the stiffening effect from shrunk-on disks. An examination of the free-free impact data would tend to indicate a 5% error limit for the test results.

Torsional Natural Frequency Accuracy

By contrast, the torsional system is closer to a pure structural model with low levels of damping commonly cited as being 2.5% modal damping or less (Wachel and Szenasi, 1993). Given an assumed accuracy of ±5%, if a TNF was predicted to have 10% separation margin, in reality the true separation margin would be between 5% and 15%. This assumed accuracy is backed by only a few comparisons between predictions and measurements of torsional systems within the literature. A sampling of the literature is presented herein.

After experiencing a torsional failure on a synchronous motor driven string (Sohre, 1965), Elliott Group performed torsional measurements to develop its first generation of criteria for torsional stress analysis. In this effort, torsional system excitation and damping were characterized and reported by Pollard, (1967). Some critical speed results from this earlier period of testing are presented herein (Pollard, 1972 and De Choudhury, 1979).

Mondy and Mirro (1982) performed torsiograph measurements on three equipment strings. Overall, the authors concluded "the error of using an undamped model to calculate the torsional natural frequencies of turbomachinery strings can be limited to less than +/-5% of the actual frequency." It should be noted that one string initially had computed errors on the order of 18%, but this was eventually attributed to poor coupling stiffness data that was later corrected.

Murray, et al., (1996) examined three different motor driven reciprocating compressor strings. Torsional prediction and measurement were conducted on two of those strings of equipment. The prediction error was 7.5% for the first string and 1.8% for the second string. The authors advocated an uncertainty analysis for torsional natural frequencies, assigning different uncertainties to the stiffness and inertia of each component. One specific study resulted in an uncertainty of -4% to +2% for the TNFs of that system.

Coupling Models

Since couplings are often the most torsionally flexible parts of the train, the torsional critical speed prediction can be particularly sensitive to their modeling. Methods for modeling couplings are discussed by Ker Wilson, (1956), Nestorides, (1958), and AGMA 9004, (2008). The 1/3 penetration rule is cited where the shaft is assumed to twist independently of the total length of the coupling (as shown in Figure 7). This "one-third" rule is applied whether the connection is keyed, splined, or interference fitted.

Calistrat and Leaseburge, (1972) examined the effect of shaft-to-hub connection and flange-to-flange connection. Their findings indicated that the torsional stiffness of hub-to-shaft connection is substantially influenced by the transmitted torque, the hub-to-shaft interference fit, and the ratio between the shaft and hub outside diameters. Rotational speed was determined to have a lesser effect. Likewise, the torsional stiffness of flanged connections can also be variable depending on the amount of bolt torque and number of bolts.

The conclusion that the modeling of fits and interfaces are critical to attaining accuracy for the torsional model is quite similar to the conclusion reached by Vance, et al. for lateral modeling (Vance et al., 1984). Steiner (2007) reported on stiffness measurements of seven couplings manufactured by three different vendors. His research suggests that contribution of disc pack and bolting to coupling stiffness may be difficult to predict. The prediction error for coupling stiffness ranged from -10.6% to +12.1%, which is within the ±20% coupling stiffness accuracy range discussed by Feese and Hill (2009). The standard deviation of Steiner's presented results ranged from ±1.9% to ±12.1%.

Torsional Measurement

As shown within the literature, torsional testing is certainly not new and it has certain advantages (Feese and Hill, 2009). In general, measurements should be more accurate than calculations especially when conducted under full load where actual response can be determined such as dynamic torque, alternating stresses, torsional oscillation, current pulsation, etc. These values can then be compared to allowable limits, and if determined to be acceptable under all possible load conditions including unloaded case, the SM would be secondary as the stress levels would be validated. Unfortunately, testing all load conditions may be difficult in a shop environment, during an outage, or while operating a plant. Some shop tests are unloaded mechanical runs, and do not use the contract driver.

Even with strain gage telemetry system, laser vibrometer, or shaft encoder only a few points can be measured within the train. Therefore, a torsional analysis is still needed to infer amplitudes at other locations that cannot be accessed for measurement. By normalizing the computer model to match the measured data (both TNFs and amplitudes) reasonable analytical accuracy can be assured such that conclusions and inferences can be drawn at the points of the system that are not directly measured.

The systems, which would benefit the most from torsional measurement, and the ones with the highest risk for torsional failure seem to be related to variable frequency drive (VFD)

applications (Feese and Maxfield, 2008, Kerkman et al. 2008, Piergiovanni et al. 2010, Kocur and Muench, 2011, and Bosin et al. 1999). The causes of these failures cited in recent literature were independent of separation margin and unpredictable in the design stage using normal methods. Each of these cases required torsional testing to solve the problem.

Accordingly, Elliott Group has performed torsional measurements both independently and with EDI. The primary reason for these measurements was to ensure a safe reliable system for the end user. Other benefits are to investigate discrepancies between measurements and predictions:

1. Different modeling methods were examined to better correlate with measurements.
2. Job coupling static stiffness was measured.
3. Other factors that might affect the coupling stiffness, such as the shrink-fit tolerance and spinning speed influences, were considered.
4. Coupling vendors were surveyed for stiffness accuracies and modeling techniques.

This paper discusses torsional error and uncertainty, and examines over ten case histories to demonstrate where variability can occur. Studies of prediction accuracy and measurement repeatability of "identical units" are provided to further a discussion in regard to a reasonable SM of both analysis and measurements.

TORSIONAL ANALYSIS

Modeling and Natural Frequency Prediction

An analytical method can be used to predict the TNFs of a machinery train. One modeling method is to use lumped inertias and equivalent torsional springs (mass-elastic model) as shown in Figures 1 and 2.
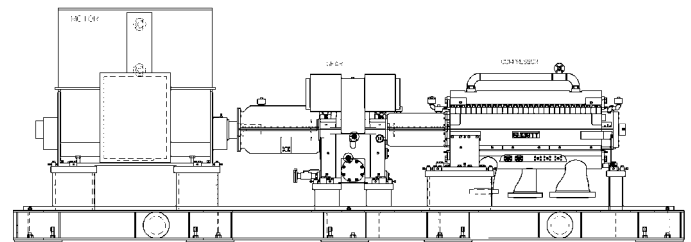

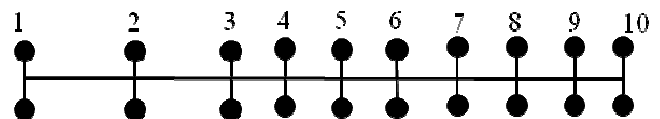*Figure 1. Motor-gear-compressor train.*

Figure 2. Lumped Inertia-Stiffness (Mass-Elastic) System.

Each component should be accurately represented in the torsional model. Guidelines for modeling each component including the couplings can be found in literature (API 684, 2005, Ker Wilson, 1956, and Nestorides, 1958). The component models can be assembled into system inertia and stiffness matrices as shown in Equation 1

$$J = \begin{bmatrix} J_1 & & & \\ & J_2 & & \\ & & \ddots & \\ & & & J_m \end{bmatrix}$$

$$K = \begin{bmatrix} K_1 & -K_1 & & \\ -K_1 & K_1+K_2 & -K_2 & \\ & & \ddots & \\ & & -K_{m-2} & K_{m-1} \end{bmatrix}$$
(1)

where m is the total number of inertias.

Note that for trains with different component speeds, the inertia and stiffness values are usually converted to the same equivalent speed before building the system matrices. However, more advanced torsional analysis programs that use full-matrix representation may be used to handle systems containing gearboxes including epicyclic gears.

An undamped analysis is typically sufficient to predict TNFs of most systems since torsional damping is usually small and on the order of 2.5% modal damping or less (Wachel and Szenasi, 1993). Some notable exceptions that are not covered in this paper include: various elastomeric couplings and fluid couplings, which have some considerable damping and non-linear behavior.

These systems of equations can be solved to determine the eigenvalues and eigenvectors (i.e., the TNFs and their corresponding mode shapes). Methods of solution include use of commercially available Eigen-solvers, such as MATLAB, or use of the Holzer or transfer matrix method (Dawson and Davies, 1975). The inertia/stiffness model can be used to calculate the vibrations if proper damping is added. The uncertainty related to different equation solvers along with the problem of root finding is not considered in this paper.

The calculated TNFs and modeshapes are typically plotted as part of the torsional report, such as shown in Figure 3.
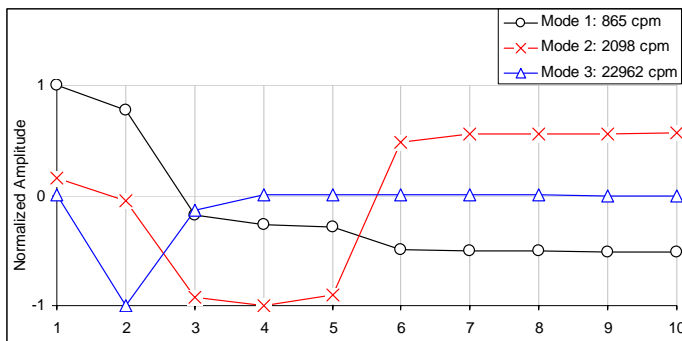

Figure 3. Torsional Mode Shapes.

Amplification Factor (AF) and Separation Margin (SM)

The calculation of AF and SM are illustrated in Figure 4, which is similar to the API lateral analysis (API 617, 2002 and API 684, 2005).
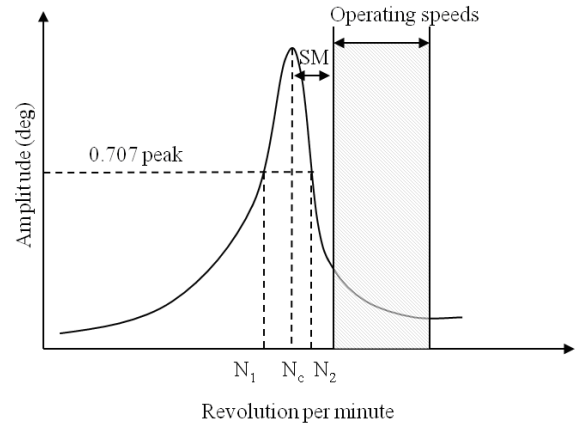

Figure 4. Torsional Response Plot.

$$AF = \frac{N_c}{N_2 - N_1}$$
(2)

$$SM = \frac{|N_{mc} - N_c|}{N_{mc}} \times 100\%$$
(3)

where N_{mc} is the speed in the operating range that is closest to N_c; usually the maximum or minimum continuous operating speed.

A typical representation of SM is the interference or Campbell diagram as shown in Figure 5.
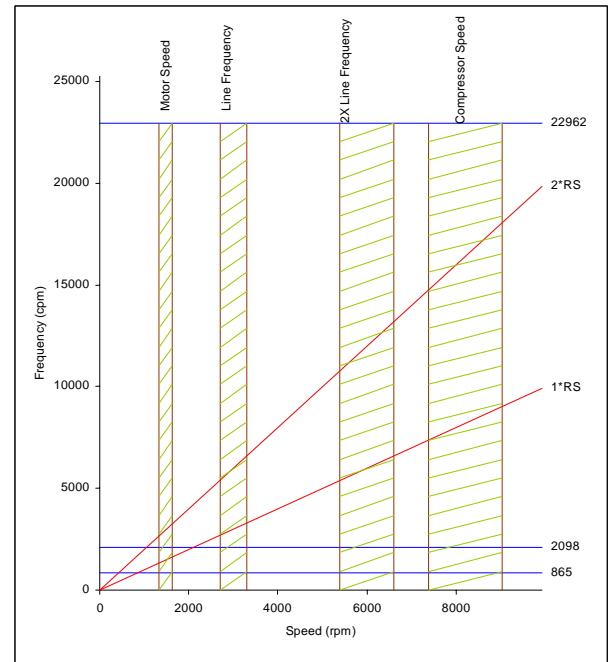

Figure 5. Interference Diagram.

Calculation of the AF is not a required part of the API 617 torsional analysis nor is it related to the SM requirement (10%). However, SM and AF are related to vibration amplitude, which can be demonstrated using a simple model.

A single-degree-of-freedom mass-damper-spring system is depicted having equation of motion as shown in Equation 4, and the gain/vibration amplitude as shown in Equation 5 (see Meirovitch, 1986 for details).

$$\ddot{x}(t) + 2\zeta\omega_n \dot{x}(t) + \omega_n^2 x(t) = \omega_n^2 A e^{i\omega t} \quad (4)$$

where ω_n is the natural frequency, and ζ is the damping ratio.

$$x(t) = A|G(i\omega)|e^{i(\omega t - \phi)}, \text{where}$$

$$|G(i\omega)| = \frac{1}{\sqrt{\left[1 - (\omega/\omega_n)^2\right]^2 + (2\zeta\omega/\omega_n)^2}} \quad (5)$$

AF is the maximum gain, i.e. $AF = |G(i\omega)|_{max} \cong \dfrac{1}{2\zeta}$ for light damping. AF is the maximum amplification of the system gain ($|G| = 1$, when $\omega = 0$), and AF is related to damping ratio. Note that the half power point (0.707 peak amplitude) method provides a good approximation of the maximum gain when the damping is small (see Ewins, 2000 for derivation/proof).

Feese and Hill, (2009) show a measured AF, and the AF for common equipment trains is between 10 and 50 (damping ratio 0.01 and 0.05). Although a very high AF of 180 was recently measured on a motor / fan system by Feese. The system gain can be calculated using Equation 5 for different speeds (different SMs), and different damping ratios/AFs, as shown in Figure 6.
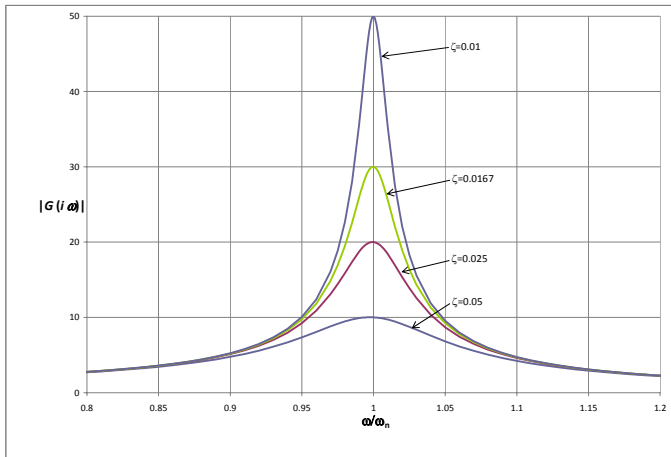

Figure 6. System Gain (AF) for Different Damping Ratios.

The numerical results in Table 1 show that for the API recommended separation margin of ±10%, amplification would be approximately 5 for most cases, and amplitudes would almost double if the separation margin was ±5% instead of the recommended ±10%. Low separation of 1% or less will increase the amplitudes significantly.

Table 1. Magnification at Different SMs and AFs.

Damping Ratio ζ	Separation Margin (SM) →				
	0%	±1%	±5%	±10%	±15%
0.05	AF = 10	10	7	5	3
0.025	20	19	9	5	4
0.0167	30	26	10	5	4
0.01	50	36	10	5	4

Uncertainties in Modeling

If the lumped inertia-stiffness model truly represents the equipment train, then the calculated TNFs will match the real system's TNFs. All factors that cause a difference between the calculated TNFs and the true TNFs of the system are considered uncertainties in this paper. There are two types of uncertainties in the modeling: errors and variations.

Error type uncertainties include:
- Mass-elastic model contains insufficient number of stations to predict natural frequencies of interest.
- Inaccurate dimensions.
- Inaccurate material properties.
- Improper modeling of complex shapes and connections, such as motor core.
- Improper modeling of components, such as not including entrained fluid in wet impeller inertia.
- Misapplying the 1/3 penetration rule or neglecting it.
- Assuming too much damping thus making predicted torsional response unrealistically low.
- Unit conversion – English versus SI.
- WR^2 versus GD^2. GD^2 is based on diameter such that $GD^2 = 4WR^2$.
- Manufacturing and assembly tolerances.

Variation type uncertainties include:
- Dynamic vs. static stiffness.
- Wear or deposit induced inertia change.
- Temperature induced stiffness change.
- Working condition/load induced stiffness change.
- Aging of material induced stiffness change.
- Wearing, cracking or damage induced stiffness change.
- Variation of shaft positioned in coupling hub.
- Variation in shrink fit.
- Variation in bolt torque.

Among all the error type uncertainties, one common concern is the shaft end modeling for penetration type of couplings. Most coupling vendors consider the shaft end, which is inside of the coupling, as part of coupling when calculating the coupling stiffness, i.e., the 1/3 penetration rule in Figure 7. However, different motor/gear vendors quite often provide the torsional stiffness differently. Figure 7 (a) shows the correct use of torsional stiffness: from the last inertia location to the start of the coupling. Figure 7 (b)-(e) show other ways that torsional stiffness is provided.
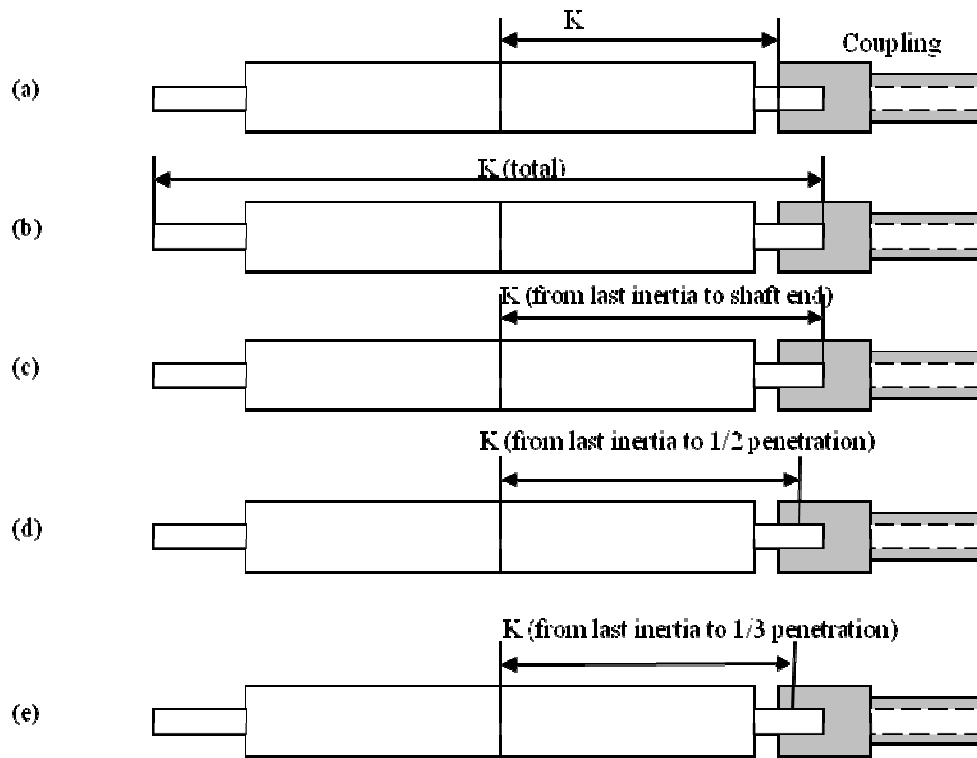
Figure 7. Vendor-provided Torsional Stiffness.

Since the shaft ends are the weakest part of the body, the stiffness provided in different ways could have large differences. When conducting the torsional analysis, the penetration factor needs to be carefully considered.

If correctly modeled, the uncertainties of the inertia of all bodies including couplings are considered within 5% (see Murray et al. 1996 for example). The stiffness of motor/gear/compressor is also considered accurate for most applications, usually within 5%. The coupling stiffness is the least accurate and also most influential to the TNFs since they are the weakest parts in the equipment trains.

For coupling uncertainties, both error type and variation type uncertainties are significant. Comparing to a rotor shaft, the coupling structure is much more difficult to be accurately modeled. Besides following API Standard 671, (2010) and AGMA 9004, (2008) coupling vendors also use FEA analysis to optimize the design and calculate the stiffness. Some manufacturers conduct tests to verify their own empirical stiffness calculations. However, even with all the standards, FEA analysis, large amount of tests, and strict rules for installation etc., for most vendors the uncertainty/accuracy of the couplings is still about 15-25%, and the estimation is based on static test only (see Table 2).

The reality could be even worse for the coupling stiffness accuracy because of the variations. For instance, load condition can be a key factor for the torsional stiffness of disc type of couplings because of the buckling effect (Steiner, 2007). The buckling effect makes the stiffness vary due to the load condition and history (see Figure 8). Vendors usually provide the coupling stiffness based on the rated/normal torque, so if the working condition is different, the torsional stiffness could be 20-30% different from the designed value, which already has 15-25% uncertainty. An example of TNF measurement can be seen in Figure 9 (the first TNF shifted 3%).

Rotation is known to affect the coupling stiffness in the axial direction, but the influence for the torsional stiffness is not well established in the literature. An FEA study was conducted on a case for which the axial stiffness changes 1/3 due to the rotation, and the results show that the influence on the torsional stiffness is negligible.

Aging of materials, including erosion/corrosion etc., could be a major problem for certain type of couplings, such as elastomeric type, so it needs to be considered at the design stage.

Influence of Uncertainties

With the estimation of the uncertainties for each component, it is possible to evaluate uncertainties in the predicted/calculated TNFs.

Motor-gear-compressor trains are a common torsionally concerned category. This paper conducted a study on TNFs using seven shop orders of motor-gear-compressor trains whose TNFs have all been measured (all with partial or no load). Some parameters are listed in Table 3. Two studies were performed with these shop orders.

First Study – Sensitivity

A sensitivity study was performed by varying each parameter sequentially, such as the inertia of the motor or the stiffness of a coupling, to see the change in the calculated TNFs. The purpose is to find whether discrepancies between prediction and measurement are related to parameter variation.

The simulation is done by applying 1% variation to the inertia of the motor, gear, compressor, and the stiffness of the two couplings. The results are shown in Table 4, where I_{1-4} stands for the inertia of the motor/gear/compressor/turbine, and K_{1-3} represents the torsional stiffness of the couplings. The predicted and measured values are listed for the coupling modes of each shop order. In some cases, the 2nd TNF could not be measured.

The sensitivity study results, such as *-0.35% and 0%* in the table for S.O.1 in column I_1, are calculated as: use +1% inertia for the motor and keep all other inertias and stiffness unchanged, calculate the TNFs (*new TNFs*), and the difference between the *new TNFs* and the predicted for 1st and 2nd TNFs are listed as *-0.35% and 0.00%*. Similar calculations were carried out for all other numbers.

Several points can be drawn from Table 4:

1. Increasing the inertias always decreases the TNFs. Usually they affect the coupling mode which is next to them, e.g., the motor affects the motor-gear coupling mode.
2. Increasing the coupling stiffness always increases the TNFs. Usually the first coupling mode is the one between the large inertias, e.g. motor and gear.
3. When the coupling sensitivity is within ±0.3%, the discrepancies between the predictions and measurements (prediction errors) are within 5% for the thirteen listed cases, which were all API turbomachinery strings.

The first two points are straightforward, i.e., the systems might be complicated but the basic physics works the same. The third point, relationship between sensitivity and prediction errors, needs more data to determine if this relationship will hold for other cases, and especially other types of strings.

Second Study – Worst Case Scenario

S.O.1-7 (M-G-C) and S.O.9 (T-C-M, i.e. no gear) are used for the second study, estimating the worst case scenario. Assume the uncertainties of all inertias are within 5%, and uncertainties of all stiffness are within 5% except for the coupling stiffness. Two sets of uncertainties of the coupling stiffness are used, 15% and 25% (see Table 2 for reference), and the results are shown in Table 5.

The first five columns in Table 5 are the same as in Table 4. The last two columns are the differences (in absolute values) between column 3 and the calculated TNFs with the assumed uncertainties, i.e., they are the uncertainties of the predictions. The prediction uncertainties can be considered as the overall sensitivity.

Since Table 5 shows the worst case scenario, it means if the coupling stiffness has accuracy within 15%, and all other stiffness and inertias are within 5% of the real values, then predicted TNFs should be within 10% of the true values. The prediction uncertainty approaches 15%, when the coupling stiffness accuracy is within 25%.

To investigate the discrepancies, some of the torsional analyses were thoroughly checked to make sure there were no human errors present. For some of the shop orders, the motor and gear vendors were requested to confirm/verify their numbers. One coupling vendor even performed a static test to verify their predicted coupling stiffness. All checks indicated no major errors/mistakes, yet the differences are more than 10% from the measurements for some shop orders. One explanation would be the variation-type uncertainties for the couplings, especially since all tests were performed with only partial or no load. Another explanation would be that there were still human errors, since some vendors may not be fully aware of the torsional modeling techniques.

Table 2. Coupling Vendor Survey Result.

			Vendor A	Vendor B	Vendor C	Vendor D	Vendor E
Accuracy of torsional stiffness			Short: 10-25% Long: 5-15%	5%	10%	Regular: 5-10% Elastomer block: 15%	25%
Torsional stiffness test			Static testing	No in-house test	Static testing	Static testing	Static testing
Penetration model (keyed & hydraulic)			1/3 penetration				
Interference (inch/inch diameter)	Hydraulic fit		0.002-0.0025	0.002-0.0025	0.002-0.0028	0.002-0.0028	0.002
	Keyed	Straight	0.0005-0.00075	0.0005	0.0005	0.0005-0.00075	0.0005-0.00075
		Taper	0.001		0.001	0.001	

Table 3. Parameters of the Geared-compressor Trains.

Shop Order	Start Year	Driver Rated Power (HP)	Driver speed (RPM)	Gear Ratio	Train Type[1]
S.O.1	2010	11000	1000-1550	8.03	M-G-C
S.O.2	2009	4000	1200-1600	6.55	M-G-C
S.O.3	2009	4000	1200-1600	8.19	M-G-C
S.O.4	2009	9300	1450-1900	5.32	M-G-C
S.O.5	2009	13000	1400-1900	4.93	M-G-C
S.O.6	2009	12000	1400-1900	2.86	M-G-C
S.O.7	2009	1770	1400-1880	3.35	M-G-C
S.O.8	2005	1350	1040-1559	7.5588	M-G-C
S.O.9	2003	16200	3420-3636	1	T-C-M
S.O.10	2003	16200	3420-3636	1	T-C-C-M
S.O.11	1971	39793	3465-4851	1	T-C-C-C
S.O.12	1979	3485	5266-7899	1.4544	T-G-C
S.O.13	1977	6000	1800	4.2644	M-G-C

---

1 Trains are listed from driver to driven side. M means motor if on driver side (such as M-G-C), and means motor/generator if on driven side (such as T-C-M/G). G means gear, C means compressor, and T means turbine.

Table 4. Sensitivity of TNFs to the Change of Inertia Stiffness.

Shop Order	Predicted TNF No.	Predicted TNF (Hz)	Measured TNF (Hz)	Difference (%)	Sensitivity of +1 percent change (%) I_1	I_2	I_3	I_4	K_1	K_2	K_3
S.O.1	1st	15.1	17.2	-12.21	*-0.35*	-0.12	-0.02		0.37	0	
	2nd	58.7	57.5	2.09	*0.00*	-0.07	-0.42		0.00	0.38	
S.O.2	1st	15.8	17.2	-8.14	-0.35	-0.04	-0.1		0.38	0.04	
	2nd	32.7	32.2	1.55	-0.01	-0.25	-0.23		0.04	0.41	
S.O.3	1st	15.2	16.2	-6.17	-0.34	-0.14	-0.02		0.40	0	
	2nd	64.9			0.00	-0.06	-0.41		0.00	0.43	
S.O.4	1st	19.4	21	-7.62	-0.19	-0.26	-0.04		0.41	0	
	2nd	72.5			0.00	-0.07	-0.4		0.00	0.41	
S.O.5	1st	20.8	23.6	-11.86	-0.25	-0.20	-0.04		0.38	0	
	2nd	71.8			0.00	-0.07	-0.41		0.00	0.33	
S.O.6	1st	16.1	15.5	3.87	-0.29	-0.01	-0.2		0.24	0.13	
	2nd	37.6	36	4.44	-0.02	-0.39	-0.08		0.10	0.3	
S.O.7	1st	11.8	12	-1.67	-0.35	0.00	-0.15		0.28	0.16	
	2nd	43.6	46	-5.22	-0.01	-0.44	-0.02		0.15	0.31	
S.O.8	1st	12	11.6	-9.43	-0.33	-0.06	-0.11		0.39	0.01	
	2nd	53.4			0.00	-0.30	-0.19		0.01	0.39	
S.O.9	1st	11.5	11.6	-1.01	-0.07	-0.08	-0.34		0.25	0.09	
	2nd	23.6	25.1	-5.84	-0.01	-0.35	-0.12		0.17	0.14	
S.O.10	1st	8.6	8.6	-0.77	-0.12	-0.08	-0.04	-0.25	0.24	0.07	0.04
	2nd	13.3	13.8	-3.98	-0.04	-0.27	0.00	-0.18	0.17	0.08	0.06
	3rd	34.8			0.00	-0.02	-0.43	-0.04	0.00	0.19	0.09
S.O.11	1st	13.2	12.4	6.72	-0.16	0.00	-0.30	-0.04	0.12	0.38	0.01
	2nd	34.0	32	6.25	-0.04	-0.20	-0.01	-0.26	0.20	0.03	0.27
	3rd	36	35.1	2.66	-0.03	-0.21	-0.06	-0.19	0.18	0.09	0.22
S.O.12[2]	1st	47.7	50	-4.57	-0.24	-0.06	-0.19		0.00	0.00	
	2nd				-0.10	-0.38	0.00		0.43	0.00	
S.O.13	1st	26.4	27.1	-2.58	-0.17	-0.04	-0.29		0.12	0.04	
	2nd	109	92.2	18.2	0.00	-0.37	-0.08		0.03	0.17	

---

2 This train has a variable speed drive, and its internal low stiffness rather than the couplings dominates the first critical.

Table 5. Worst Cases of the Predicted TNFs Due to the Modeling Uncertainties.

Shop Order	Predicted Values		Measured	Difference	Coupling Uncertainty	
	TNF No.	TNF (Hz)	TNF (Hz)	(%)	15%	25%
S.O.1	1st	15.1	17.2	-12.21	8.78	13.09
	2nd	58.7	57.5	2.09	8.91	13.36
S.O.2	1st	15.8	17.2	-8.14	9.22	13.99
	2nd	32.7	32.2	1.55	9.49	14.55
S.O.3	1st	15.2	16.2	-6.17	9.12	13.75
	2nd	64.9			9.29	14.13
S.O.4	1st	19.4	21	-7.62	9.18	13.86
	2nd	72.5			9.14	13.87
S.O.5	1st	20.8	23.6	-11.86	8.89	13.34
	2nd	71.8			8.40	12.39
S.O.6	1st	16.1	15.5	3.87	8.72	12.99
	2nd	37.6	36	4.44	9.03	13.61
S.O.7	1st	11.8	12	-1.67	9.46	14.41
	2nd	43.6	46	-5.22	9.54	14.63
S.O.9	1st	11.5	11.6	-1.01	8.13	12.16
	2nd	23.6	25.1	-5.84	8.05	11.57

Table 6. Comparison of Measured and Calculated TNFs.

System	First TNF			Second TNF		
	Measured	Calculated	Percent Error	Measured	Calculated	Percent Error
1600 kW	720 CPM	686 CPM	-4.7%	2760 CPM	2570 CPM	-6.9%
7000 kW	1260 CPM	1165 CPM	-7.5%	--	4347 CPM	--
11,500 kW	930 CPM	968 CPM	+4.1%	2,160 CPM	2,257 CPM	+4.5%

Torsional Measurement

According to API 684, 2005, a torsional analysis should always be performed for new designs. However, other industries do not require this and unfortunately, torsional vibration might not be considered to be a problem until after a failure has occurred. Situations where torsional testing may be required in addition to a computer analysis include:

- **Troubleshooting torsional failures** – If an unexpected or premature failure of a component occurs, testing of the repaired system is often the best method to fully investigate the cause(s) of the failure.

- **Critical applications** – If a system poses unusually high risks to life, other machinery, or plant processes, testing should be performed to ensure reliable operation. This could include a prototype machine or a re-rated model operating at higher speeds or pressures than previously designed.

- **High chance of variability** – This could include systems with torsionally soft couplings and/or wide speed ranges or operating conditions. If many assumptions had to be made in the analysis phase due to lack of shaft drawings and technical information,

testing should be performed to verify the analytical results.

- **Product development** – Newly designed systems that will be mass produced should be tested under load. It is much easier to correct a problem with an initial unit at the factory than it is to retrofit many units that have already been shipped to customers and installed in the field.

- **Used systems** – Compressor systems that have been modified or put into a different service, such as re-staging and/or changing operating conditions, should be re-analyzed or tested.

- **Contractual Requirement** – Some municipalities have specifications that require torsional vibration testing of new units by a professional engineer during commissioning. Some end users also require full-load, full-string tests of their equipment at the shop if possible or during commissioning at the plant. Torsional testing is a bulleted item within the API specifications indicating that it is an option that can be selected.

Torsional vibration is referred to as "silent" because it occurs in the axis of rotation, which conventional vibration monitoring equipment, such as accelerometers and proximity probes, may not normally detect. Therefore, special test equipment is needed to measure torsional vibration as discussed in the APPENDIX. One exception is gearboxes where dynamic torque produces varying tangential and separating forces between the gears and fluctuating loads on the bearings, which can produce noise. Coupling chatter, disc pack deformation, damaged rubber elements, damper failures, and compressor oil pump failures are possible symptoms of a torsional vibration problem.

Test Conditions

The TNF might change under various load conditions. A major factor is the torsional stiffness change of the couplings. Figure 8 shows the test results of static load versus angle of a disc-type coupling.
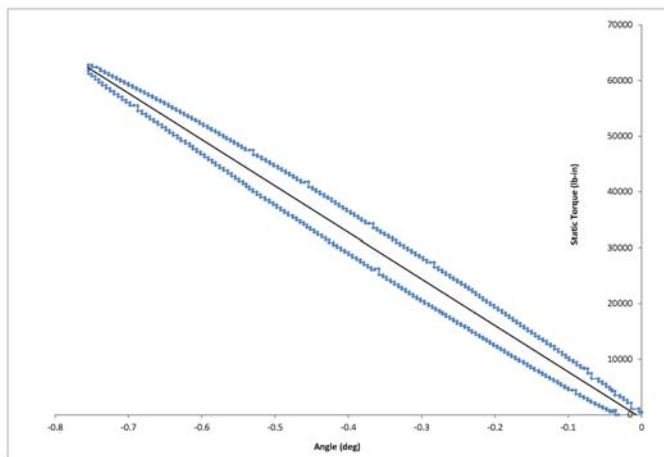
Figure 8. Static Load Test of a Disc Coupling.

Under different loads, the coupling stiffness could change 20-30%. Figure 9 shows the measured torsional vibration, and the first peak shifts approximately 3%.
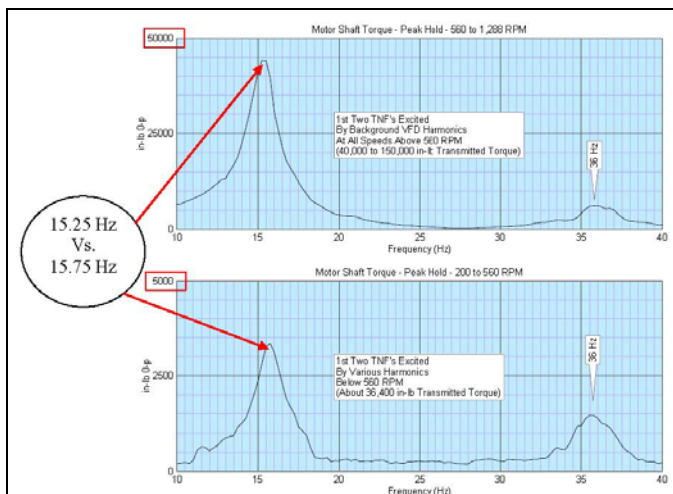
Figure 9. TNFs under Different Load/Torque Conditions.

For unloaded shop tests (centrifugal compressor operating under vacuum), it is best to collect data during a continuous ramp up in speed. This helps to ensure that the gear teeth remain in contact due to torque required to accelerate the inertia of the high-speed compressor. When the gear teeth momentarily separate or backlash, the TNFs will change and the steady-state model for the entire train will be invalid. For one case, the TNFs of the low-speed side and high-speed side were shown to match the modeling if analyzed decoupled (zero stiffness at the gear mesh).

Waterfall plots of frequency spectra (i.e. Figure 21) are good for displaying multiple harmonics over a speed range. Peaks often indicate resonant conditions. Order tracking can also be used to separate responses at the various harmonics. Phase angles can be determined from a once-per-revolution tach signal and used to confirm a phase shift through a suspected resonance as shown in Bode plots.

For systems without a gearbox, the TNFs and damping can sometimes be measured from the time wave forms after a trip event. Suddenly removing the power to the motor can cause a torque impulse and "ring" the system.

An example is shown in Figure 10. By examining the period of vibration, the first TNF was approximately 15 Hz. The damping can be determined from the logarithmic decrement, δ, which was approximately 0.44. This converted to a damping ratio ζ of 0.07 and an amplification factor AF of approximately 7 (see Randall, 1990 for detailed explanations). This system had a VFD motor and MVR (mechanical vapor recompression) fan with a rubber coupling, which had a reported dynamic magnifier of 8. Therefore, the measurements confirmed the analytical results.
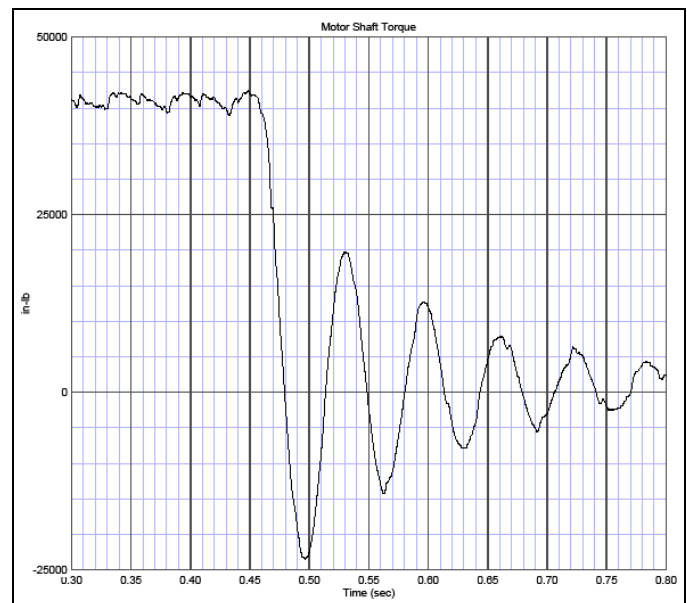

Figure 10. Free Torsional Vibration after Trip Event.

ACCURACY OF PREDICTIONS

Motor – Gearbox – Compressor Systems

The systems consisted of a motor, speed increaser, and centrifugal compressor as shown in Figure 11. The end-user requested that torsional measurements be taken on several compressor systems to verify the torsional natural frequencies.

These measurements were performed during mechanical runs at the shop. The strain gage telemetry system was installed on the LS coupling as shown in Figures 12 and 13.
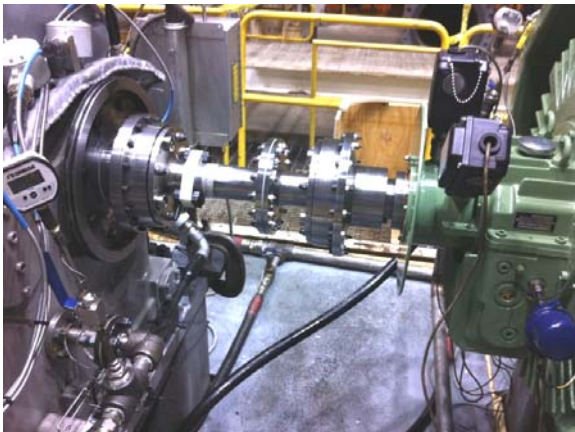

Figure 11. Compressor System.

Figure 12. Low-Speed Coupling

Figure 13. Strain Gage Telemetry System.

The motor speed was controlled by a VFD and the compressor was operated with a vacuum (no load). By accelerating the unit, the gear teeth would maintain sufficient contact.

The first and sometimes second TNFs could be determined from the measured data. Table 6 shows how the torsional analyses agreed with the actual TNFs that were measured for each system.

Differences are attributed to coupling stiffness and/or simple motor model provided. It is believed that the accuracy of the predictions could be improved with coupling test data and multiple-station model for the motor core (Hudson and Feese, 2006). Load may also change the torsional stiffness of the shim pack couplings slightly.

Note that the 1600 kW system originally was found with a much lower first TNF. Upon inspection, the motor shaft diameter was undersized. This was corrected by manufacturing a new motor shaft. Test results presented are for the correctly sized motor shaft, which was later re-tested.

Effluent Pump System

The incoming water to the facility is primarily from storm sewer drainage. The volume of water handled varies widely from storm conditions to dry periods. The treated water is discharged to the Pacific Ocean; therefore, the pump head requirements depend on the tide as well as desired flow. The effluent pump has a maximum capacity of 68.5 million gallons per day (MGD), and 90 feet of head.

As shown in Figure 14, the system uses a double input, right-angle gear reducer with a diesel engine with clutch on one input shaft and a VFD motor with clutch on the other input. The pump system is designed such that only one clutch is engaged at a time. The vertical pump is driven by the gear output shaft. The torsional natural frequencies of the system change due to different drivers being engaged or disengaged.

Figure 14. Water Pump System.

VFD Motor Operation

With the VFD motor in operation, a torsional natural frequency (TNF) was measured at 12 Hz, which compares with 9.5 Hz from the original torsional analysis. Another TNF was measured at 170 Hz with the pump strain gages, which compares with a calculated mode at 143 Hz. From strain gages on the motor shaft, a TNF was found at 110 Hz, which compares to a predicted value of 124 Hz.

Engine Operation

With engine operation, the initial torsional response was 8.5 Hz, which compares with predicted 7.3 Hz (engine warm-up / clutched disengaged). During the speed sweeps, a TNF was measured at 10 Hz, which compares with 11.8 Hz from the original torsional analysis. Two other TNFs were measured at 65 Hz and 85 Hz. These compare with the predicted values of 70 Hz and 89 Hz.

There were many possible variations in the system. For example, the coupling mounted to the engine flywheel contains rubber elements in shear. The stiffness properties of the rubber elements can vary by up to 25% from the published values due to age hardening or other factors. For example, temperature of the blocks could affect the first TNF; colder elements will be stiffer than warmer elements. In addition, the stiffness of the clutch is affected by the air pressure, which clamps the element and drum together.

It is interesting to note that the specification for this project required three independent torsional analyses be performed in the design stage and that all three analyses had to agree within a few percent on the TNFs to be accepted. Even after all of that effort, the measured results were substantially different from the predicted frequencies. However, several important upgrades were recommended in the design stage as a result of the torsional studies, which included using higher strength shaft materials for some parts.

This was an extremely complicated system with various operating conditions and wide speed ranges. Therefore, it was impossible to satisfy the contract specification, which required that no torsional critical speeds be within the range of 20% below the minimum speed to 30% above the maximum speed. This was a much larger SM than the 10% required by API. Therefore, it was recommended that one pump system be tested during commissioning to confirm the resonant speeds and stresses by measurement.

Both the engine and VFD motor were tested. Switching back and forth between these two drivers while operating the pump was performed smoothly due to the excellent control system. Therefore, the system was verified to be acceptable. It was possible to have acceptable torsional vibration without satisfying the SM required because of the rubber coupling mounted on the engine flywheel, which provided damping, and the smooth VFD with low torque ripple (less than 1.5%). The gearbox was rated up to 40% dynamic torque.

It is interesting to note that the second author was recently involved with another engine – gearbox – vertical pump system that experienced multiple line shaft failures at the keyway. These failures are believed to be caused by sudden engagement of the clutch between the engine and gearbox when the engine is already at a high idle speed. Although not typical torsional vibration, it is important that sudden torque spikes not be introduced into the system that could yield the shaft material at geometric discontinuities such as keyways and /or damage gear components.

Sewer District – Pumping Station

The system consisted of an induction motor, rigid coupling, and vertical centrifugal pump as shown in Figure 15. The motor was rated for 1750 HP at 400 RPM. A new VFD was being installed in order to operate the pump from 270 RPM to 400 RPM and needed to be evaluated.

Figure 15. Vertical Motor - Pump System.

The first TNF was predicted to be 31.8 Hz with the torsional analysis. A simple lumped parameter mass-elastic model was used. Later, the first TNF was verified to be 31.9 Hz using strain gage telemetry system in the field. This was nearly perfect agreement with less than 1% error.

To achieve good agreement, it is important to use the correct pump impeller inertia. Entrained fluid will add to the WR^2 value and is commonly referred to as the wet inertia value. Solid modeling can be used to calculate the inertia of the water within the impeller. Charts are available to estimate the extra inertia depending upon the impeller type and diameter. If actual dimensions are unavailable, then a general rule of thumb is to assume an additional 25% inertia to account for entrained water in the impeller.

Mixed Refrigerant Compressor Train for LNG Project

A torsional analysis of the system was performed by the pump manufacturer. Measurements were later taken. A comparison is shown in Table 7 below.

Table 7. Calculated and Measured TNFs.

Mode	Calculated		Measured		% Diff
1	605	CPM	618	CPM	2.1%
2	1159	CPM	1320	CPM	12.2%
3	1632	CPM	1638	CPM	0.4%
4	2581	CPM	2268	CPM	13.8%

As shown in the table, the first and third TNFs had good agreement. However, the second and fourth TNFs had more than 12% difference. If the torsional mode shapes were examined in greater detail, it may have been possible to determine, which components had erroneous mass-elastic data.

Motor Driven Compressor System

The compressor system consisted of the following:

- Induction motor, rated 400 HP (298 kW) at 595 RPM
- Disc pack coupling - hub on motor side and adapter on compressor side
- Flywheel mounted to compressor crankshaft
- Reciprocating compressor with two throws

A torsional analysis was performed in the design stage. The coupling size was selected based on proper service factor. The flywheel was sized to tune the first TNF between compressor orders. For this case, the first TNF was predicted to be 55 Hz, which would be between 5× and 6× compressor speed. The second TNF was predicted to be above 30× running speed and therefore not considered a problem.

Because of previous concerns with coupling stiffness values provided by the manufacturer and the criticality of tuning the first TNF between harmonics to avoid high torsional vibration, measurements were recommended. A strain gage telemetry system was mounted to the motor shaft extension. The first TNF was determined to be 59 Hz instead of 55 Hz as predicted.

The percent error is approximately 7%, which is not that far from the expected range of ±5%. However, the first TNF is now only 1% from the 6× harmonic and electrical frequency of 60 Hz. This is much less than the API recommended separation margin of 10%. For this particular system, it would not be possible to achieve a 10% separation margin from both 5× and 6× compressor harmonics even if the actual TNF had been 55 Hz as predicted.

The compressor system was tested over all load conditions and found to still have acceptable stress levels in the motor shaft and dynamic torque in the coupling. However, the safety factor was reduced to less than two, which is normally used in the analysis during the design stage. To understand what may have happened, the torsional mass-elastic model must be normalized to match the measured field data.

Parametric studies were performed one at a time to determine the sensitivity of each component on the first TNF. In general, the torsional stiffness must be higher or the inertia must be less than used in the analysis in order for the first TNF to be greater than predicted (59 Hz instead of 55 Hz). Results are summarized in Table 8.

Table 8. Results of Parametric Study.

Component	Percent of Given Value
Motor Inertia	75%
Motor Core Stiffness	Insensitive
Motor Ext. Stiffness	125%
Coupling Stiffness	180%
Flywheel Inertia	75%
Compressor Inertia	Insensitive
Compressor Stiffness	Insensitive

Variations in a range from 30% to 300% of the given values were examined. As shown in Table 8, the system is most sensitive to motor and flywheel inertia as well as motor shaft extension stiffness. There is some sensitivity to the coupling stiffness, but essentially no sensitivity to motor core stiffness and mass-elastic properties of the compressor.

To explain this, the percent strain energy and kinetic energy for the first torsional mode were calculated. Results show that 65% of the strain energy is in the motor shaft extension and 30% is in the coupling. Therefore, these are the most sensitive components in terms of stiffness. Results show that the motor core and flywheel each have approximately 47% kinetic energy for the first torsional mode. This makes both of these components the most sensitive from an inertia standpoint.

The flywheel inertia calculation is straight forward and should therefore be accurate. The compressor inertia and stiffness were shown not to affect the first TNF. So for this system the uncertainty is most likely with the motor inertia and stiffness. Unfortunately, since the system was installed, there was no practical way to verify motor dimensions, weights, etc.

The coupling stiffness could also affect the results, but would need to have a larger percentage of error (80% for the coupling versus only 25% for the motor). It was unknown if the coupling manufacturer had actual factory test data to substantiate the provided value.

This particular system had a heavy shrink fit on the coupling hub, small diameter motor shaft, and no keyway. It is interesting to note that if the 1/3 rule is omitted, then the calculated first TNF would match the measured value. Ignoring the penetration effect would be equivalent to modeling a stepped shaft.

Example of Error Due to Torsional Stiffness of Coupling

Multiple disc pack coupling failures were caused by high torsional vibration due to insufficient separation margin from a compressor harmonic (multiple of running speed). All of the six-throw reciprocating compressors were driven by 8000 HP (5966 kW) synchronous motors at a constant speed of 720 RPM. The same model flexible disc couplings were used on all units between the motor shaft and compressor flywheel.

Units that experience coupling failures had the same brand

motors. The first TNF was predicted to be 3203 CPM (53.4 Hz). Measurements showed the actual frequency to be 58.5 – 60.5 Hz on the three units tested. Analysis error was approximately 9% to 12% and the separation margin was non-existent from the 5× compressor harmonic.

Other units with no reported coupling failures had another motor brand and different size flywheel driving the same model compressor. For these units, the first TNF was predicted to be 3186 CPM (53.1 Hz). Measurements showed the actual TNF to be 57 Hz, with approximately 7% analysis error. Results showed the SM was actually 5% instead of 11% as predicted.

Originally, an independent consultant was requested to perform a torsional analysis of reciprocating compressor trains. The flywheel was sized for each motor to tune the TNFs. However for reciprocating equipment, it is difficult to avoid all harmonics by the recommended 10% separation margin. For example, the first five compressor orders are: 12 Hz, 24 Hz, 36 Hz, 48 Hz, and 60 Hz. Perfect tuning between 4× and 5× would be 54 Hz resulting in an 11% separation margin.

Because there was insufficient separation margin from 5× running speed, the dynamic torque in the coupling was much higher than predicted. Measured values exceeded the coupling manufacturer's allowable level. This is considered the root cause of the shim pack failures.

By comparing the two torsional models, it was concluded that the most likely cause of these errors was the torsional stiffness value provided for the coupling, which was common for all units. Both torsional models were normalized by increasing the coupling stiffness by approximately 50%. A simple hand-calculation showed that the stiffness of the coupling could be higher and that the shim packs could be the controlling factor. It was later discovered that static test data was unavailable for the shim packs used for this size coupling.

Uncertainty Associated with Disc Pack Coupling

A typical coupling would consist of: hubs, disc packs and spacer. The coupling spacer should be the easiest to model (low uncertainty), followed by the hub and shaft penetration, and the most difficult calculation are the disc packs, which are non-linear with load and difficult to model even with finite element analysis (high uncertainty).

The 1/3 penetration rule is commonly used. Nestorides (1958) discusses this assumption, but does not provide an estimated accuracy. Various geometries such as shrink fit, keyed shafts, and tapered shaft could affect results. Therefore a "medium" level of uncertainty was placed on the 1/3 rule.

Based on this simple assessment, it would seem that when the coupling spacer is torsionally much softer than the disc pack, uncertainty of the overall coupling stiffness will be relatively low (example shown in Figure 12). However, when the spacer is torsionally stiff relative to the disc pack and no

hub (flanged directly to flywheel therefore no 1/3 rule), uncertainty could be much higher than normal as shown in Figure 16. In the second example, the disc packs control the overall torsional stiffness of the coupling and are the most difficult to predict. Due to the high torsional stiffness of the larger coupling, it may be difficult for the manufacturer to test.

Figure 16. Disc Pack Coupling with Stiff Spacer.

For critical systems that are sensitive to coupling stiffness, the value needs to be accurate. Vendors with shop test data will have less uncertainty associated with this value. For large couplings, the foundation in a test facility may not be stiff enough to apply significant torque and remain relatively rigid. Others have proposed dynamic testing of couplings to improve accuracy of torsional predictions.

Variation Among "Identical" Units

From the previous example, the compressor crankshafts were retrofitted with additional inertia (sometimes called donuts) to compensate for the higher coupling stiffness. Table 9 summarizes the first two measured torsional natural frequencies (TNFs) for multiple units tested. Note there was very little variation among the units (average value of first TNF was 53.75 Hz ±1% and having a standard deviation of 1%).

Table 9. Summary of Measured Results

Unit	First TNF	Second TNF
Station "C"		
1	54.5 Hz	80 Hz
2	53.5 Hz	80 Hz
3	54.0 Hz	80 Hz
Station "W"		
1	53.5 Hz	80 Hz
2	53.0 Hz	80 Hz
3	54.0 Hz	80 Hz

Table 10. Calculated Torsional Natural Frequencies

Torsional Mode	Original Analysis 1957 Report	EDI Torsional Analysis w/ Disc Cplg		Amplification Factor	Description
1	--	2.65 Hz	159 CPM	5	Damper Mode
2	872 CPM	14.6 Hz	875 CPM	27	Twisting Through Quill Shaft
3	2,152 CPM	35.2 Hz	2,112 CPM	10	First Engine Crankshaft Mode
4	3,020 CPM	49.7 Hz	2,981 CPM	30	Quill Shaft, Gears, Compressor

The target for the first TNF was 54 Hz, which is half-way between 4× (48 Hz) and 5× (60 Hz) compressor harmonics. The second TNF was measured at 80 Hz, which is 6.7× compressor speed. The separation margins of 10% for the first TNF and 5% for the second TNF are considered acceptable. By properly tuning the TNFs, the units have been running satisfactorily.

Engine – Gearbox – Compressor

Torsional measurements were performed on engine – gearbox – compressor units for a gas pipeline transmission station. The engine speed could vary from 430 RPM to 500 RPM. The original torsional analysis was performed by Nordberg in 1957 and did not include the separate viscous damper ring on the engine. The mass-elastic model was modified to include the new couplings and viscous damper. The first four TNFs are listed in Table 10.

EDI performed a field study to investigate the cause for crankshaft failures that occurred in the Nordberg engines. From the torsional measurements and calculations, it was determined that the crankshaft failures were due to a torsional resonance caused by the third torsional natural frequency (engine crankshaft mode) being excited by the 4.5× engine order combined with a failed engine damper.

Without the engine damper operating properly, the stress levels in the engine crankshaft were excessive when operating near resonance. The torsional natural frequency of concern is the third mode, excited by 4.5× engine speed.

Table 11 shows a variation of 33.8 Hz – 35.6 Hz for the first TNF. The average TNF was 34.9 Hz with a standard deviation of 1.8% and having total variation of 2% to 3%.

Table 11. Comparison of TNFs Measured

Unit	Frequency (Hz)	Speed (RPM)
Station "H"		
1	34.5	460
2	34.5	460
3	35.3	470
4	33.8	450
Station "D"		
1	35.6	475
2	35.2	469
3	35.3	471

With the engine damper functioning properly, operating throughout the entire speed range does not pose a problem for the system; therefore, it is very important to check the viscous dampers on a periodic basis. When the dampers are located inside the engine frames, they can be subjected to elevated temperatures and sometimes overlooked during routine maintenance (Feese and Hill, 2009).

Measurement vs. Predictions

As a summary of the comparison between measured and predicted TNFs, 41 cases are presented in Figure 17. The X-axis is the order of the TNF, i.e., 1st TNF, 2nd TNF, etc. The Y-axis is the difference in percentage of the predicted TNFs versus measured TNFs. Due to measurement difficulties, 2nd and 3rd TNFs are sometimes not measured.
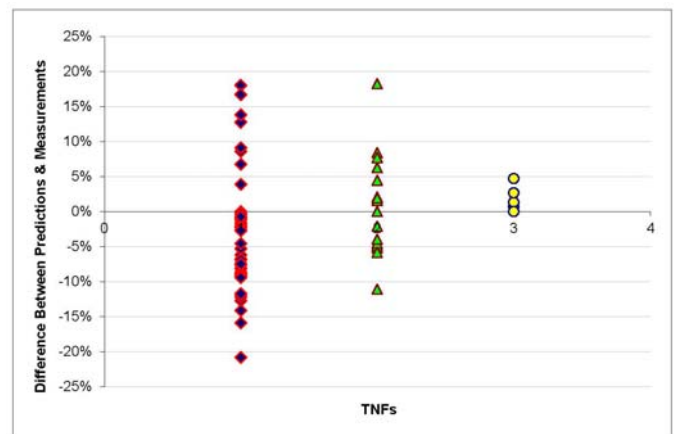

Figure 17. Discrepancies between Prediction and Measurement

The distribution of the discrepancies is summarized in Table 12, where for instance, 90% of all data points for the first TNF are within ±15%.

Table 12. Percentage of Discrepancies

TNF	within ±25%	within ±20%	within ±15%	within ±10%	within ±5%
1st	100%	97.5%	90%	70%	30%
2nd	100%	100%	93%	87%	53%

CASE HISTORIES – VFD TORSIONAL PROBLEMS

To avoid torsional vibration problems, API requires a 10% SM. This is impractical for systems with wide operating speed ranges. Sometimes special couplings are needed or skip frequencies must be programmed into the VFD. There are still other cases where the equipment trains had separation margins of 10% or more, but still suffered torsional failures.

Case History 1: Torsional Vibration Problem with VFD Motor / ID Fan at an Oil Refinery

An induced draft (ID) fan system at an oil refinery experienced a failure of the spool piece in the flexible disc coupling between the motor and fan shafts. The fan system is part of an atmospheric furnace that heats approximately 152,000 barrels of crude oil per day. The ID fan is driven by a 350 HP induction motor (Figure 18). To improve efficiency, the fan speed is varied instead of using inlet dampers to control the exhaust flow from the furnace. The motor speed is controlled by a low-voltage variable frequency drive (VFD) from 0 to 1200 RPM. Any unscheduled downtime would be costly and could quickly outweigh the energy savings from using the VFD instead of inlet dampers. Therefore, it is imperative that the system have high reliability.

Figure 18. ID Fan and Motor.

Figure 19. Cracked Coupling Spacer (Bolt Hole).

Figure 20. Cracked Coupling (Center Spacer).

The failure of the flexible disc coupling consisted of cracked space piece, which appeared to originate at a bolt hole (Figure 19). Initially, the plant maintenance was blamed for possibly over tightening the coupling bolts. However, the 45 degree angle of the crack through the coupling spacer as shown in Figure 20 is typical of high torsional vibration.

To help diagnose the actual cause of the coupling failure, field tests were performed. The torque was measured using a wireless strain gage telemetry system mounted on the motor shaft extension near the coupling hub. See APPENDIX for various methods of measuring torsional vibration. The waterfall plot in Figure 21 shows the measured frequency spectra of the alternating torque versus speed. The first TNF of the system was identified at 58 Hz.

Torsional resonances occur when energy at multiples of mechanical running speed and electrical harmonics from the VFD intersect a TNF. Because the motor has 6 poles (3 pole pairs), the mechanical frequency will be approximately 20 Hz (1200 RPM) when the fundamental VFD frequency is 60 Hz, neglecting slip of the induction motor. High dynamic torque in the coupling was found when operating the fan from 1000 to 1200 RPM due to excitation at the 1× electrical frequency of the VFD.

VFDs control motor speed by varying the electrical frequency. The VFD first rectifies the input AC power to the DC bus, then inverts from DC back to AC power at the required electrical frequency to drive the motor at the desired speed. The output frequency from the drive can range from 0 to 60 Hz. Because the output wave form is no longer a pure sine wave, torque ripple can be produced. Some newer VFD technologies such as pulse width modulation (PWM), produce smoother wave forms and thus reduced torque excitation at electrical harmonics.
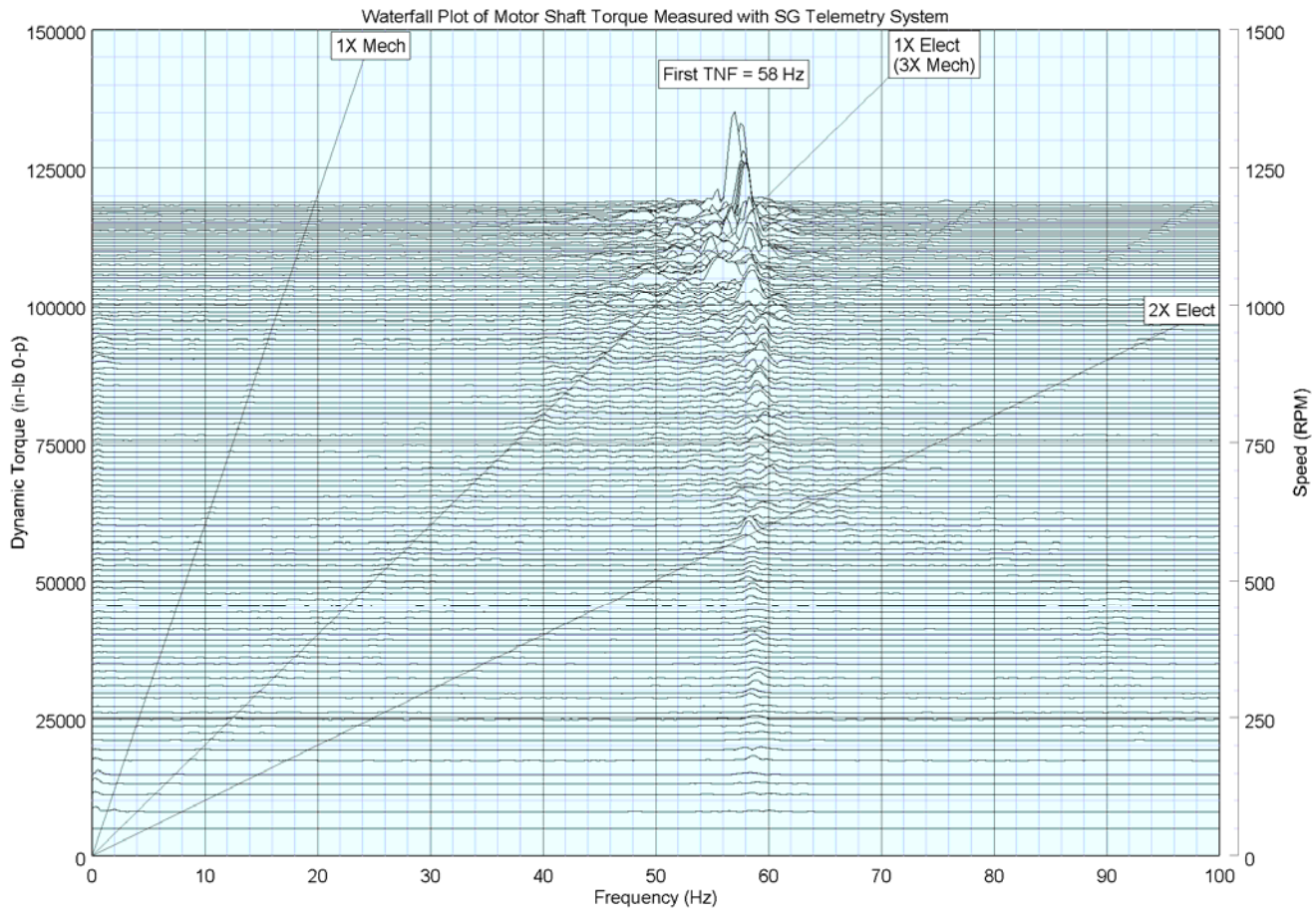
Figure 21. Waterfall Plot of Dynamic Torque.

Because the fan normally operates between 1000 RPM and 1200 RPM, which was the speed range where excessive dynamic torque occurred, this is believed to be the reason for the coupling failure. For example, the VFD excitation was approximately 5% of the full load torque (FLT) and at torsional resonance the dynamic torque is amplified by a factor of 30. Therefore, the maximum alternating torque in the coupling was approximately 150% of the transmitted torque, which exceeded the rating from the manufacturer.

Due to the large diameter and weight involved, the inertia of the fan is many times greater than the inertia of the motor. For the first torsional mode, the motor is typically near an anti-node and acts like a torsional pendulum. The fan is usually near the node and acts as an anchor. The VFD infers load changes by monitoring motor current, which could also contain variation from the first TNF. In a torsionally stiff, lightly damped system, the first TNF is very sensitive to any harmonic excitation or sudden speed adjustments from the VFD motor (Feese and Maxfield, 2008).

After further discussion with plant personnel, it was determined that the fan was originally driven by another motor from a different manufacturer. Motor repairs were needed and would take longer than acceptable. Therefore, an alternate motor was acquired and installed. The new motor from a different manufacturer was similar in electrical performance, but was vastly different in physical size and inertia.

Unfortunately, the electrical engineers did not communicate with the mechanical engineers that this change was being made and did not realize how it could impact the mass-elastic torsional system.

American Petroleum Institute (API) recommends that a torsional analysis be performed in the design stage to prevent failures. A separation margin (SM) of at least 10% between the torsional natural frequencies and the excitation frequencies is recommended to avoid running at a torsional resonance unless shown to be safe. Many times satisfying the 10% SM is impractical for VFD motor systems that operate over a large speed range.

A torsional analysis of the fan system was never performed with either motor. After the coupling failure, the motor inertia values were compared. It was found that the replacement motor had a much lower inertia (WR^2) value than the original motor. Reducing the motor inertia caused the first TNF of the system, which was originally below the minimum speed, to increase into the normal operating speed range.

Since switching back to the original motor was not an option; a temporary solution was recommended where the running speed should be limited to a maximum motor speed of 1000 RPM (VFD frequency of 50 Hz) to avoid exciting the first TNF at 58 Hz. This provided a SM of 13% between the VFD excitation frequency and the first TNF of the system.

A torsional analysis of the system was performed and normalized to match the measured field data. Based on the results of the computer analysis, an alternate coupling was selected to detune the TNF away from the 1× electrical frequency of the VFD. A coupling with elastomer blocks in compression (Figure 22) generally has a lower torsional stiffness than a flexible disc coupling and provides additional damping. The damping reduces the dynamic torque when operating near resonance. Elastomeric couplings in compression are often used on large VFD motor / fan systems found at power plants.
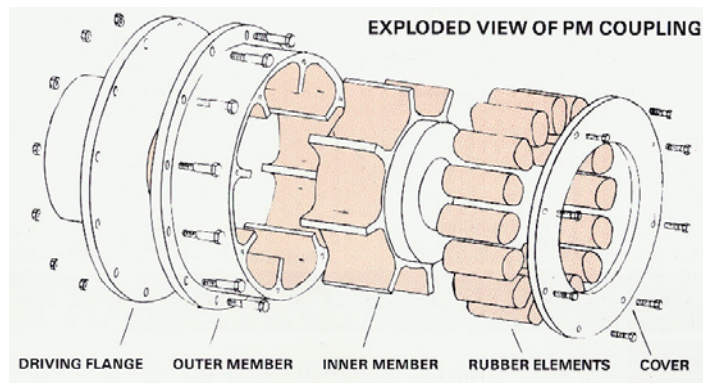
Figure 22. Flexible Coupling [Holset Catalog].

The torsional stiffness of the rubber blocks is non-linear and sensitive to shore durometer (hardness) of the rubber. Therefore when using a rubber block coupling, it is important to compute the TNFs using various rubber durometers (SM60, SM70, SM80) over the entire operating range. The interference or Campbell diagram shown in Figure 23 illustrates how the first TNF varies with speed / load for various rubber durometers. With SM60 blocks, the torsional resonance was predicted well below the normal operating speed range. Fortunately, a suitable coupling with proper size and durometer blocks was located with a short delivery time.

The coupling was installed and the fan system has been operating satisfactorily for five years. This case study shows the importance of performing a torsional analysis on a new system in the design stage and whenever the system is modified. Variables in the system include motor inertia and coupling torsional stiffness. The inertia was significantly different between the old and new motor models.

The VFD excitation was slightly higher than reported by the manufacturer. For a smooth VFD producing only 1% torque ripple, this rubber element coupling may not have been required. To achieve a reliable design, adequate safety factors must be considered to account for possible variation in the supplied information.

This case history demonstrates how important it is to perform a torsional analysis in the design stage and to have proper separation margins or to show that operating at resonance will not damage the machinery. When changes are made to the train, the torsional analysis should be revised to ensure these changes do not negatively impact the reliability.

VFD Case History 2 - VFD Motor Driving a High-Inertia Fan System with Sufficient Separation Margin

VFD motors are commonly used to drive induced draft (ID) fans and mechanical vapor recompression (MVR) fans. As previously discussed, API recommends a 10% separation margin from torsional resonance. However, VFDs are used to achieve wide speed range or to operate the motor above synchronous frequency. Older VFDs had significant torque excitation at multiples of electrical frequency (referred to as torque ripple). Avoidance using skip frequencies and/or rubber element couplings was often required to obtain a reliable system.

Newer pulse-width-modulation (PWM) drives are much smoother and can often operate at torsional resonance without creating high response. A general rule of thumb would be that drives which produce 1% torque ripple or less are considered smooth. Although electrical harmonics have been greatly reduced by these modern drives due to more sinusoidal wave forces with less distortion, increased complexity in the control system has introduced other problems. Trying to control speed to a very precise value through virtual feedback loops has been shown to cause instability in several models of low-voltage and medium-voltage drives.

The problem occurs because the high-inertia fan acts like a flywheel that does not suddenly change speeds. In fact, flywheels are commonly used on reciprocating equipment to smooth the dynamic torque in the system. Because of the large diameter size and weight involved (see reference Feese and Maxfield, 2008 for details), the inertia of the fan could be more than 20× the inertia of the motor. For the first torsional mode, the motor core is typically near an anti-node and acts like a torsional pendulum. The fan on the hand is usually near the node and acts as an "anchor". The drive calculates load changes by monitoring motor current, which could also contain variation from the first TNF. In torsionally stiff, lightly damped systems, this effect can be more pronounced.

The instability can be worse at low motor current (low load). It is believed this is because any disturbance from the TNF is misinterpreted as load change. The drive then quickly over-reacts, thus feeding the torsional amplitude. When the exhaust air from the boiler is hot, the air density will decrease, and so will the fan load of an ID fan.

In the case study from Alexander, et al., (2010), the instability occurred at a VFD operating frequency 20% - 30% above the first TNF, which was well outside the API separation margin of concern; therefore, a steady-state analysis performed according to API would not predict or prevent this type of torsional problem. Therefore, the VFD must be properly tuned during commissioning.
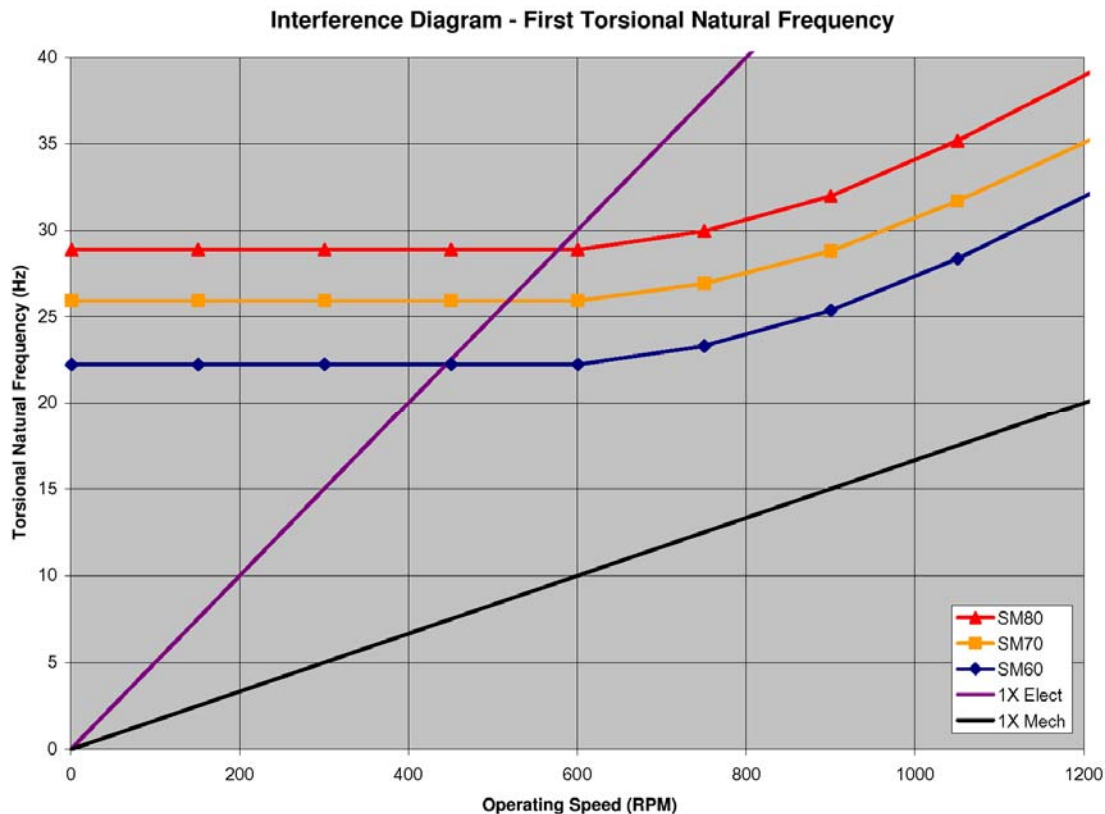
Interference Diagram - First Torsional Natural Frequency

Figure 23. Campbell Diagram.

Case History 3:   VFD Motor / High-Speed Compressor at Chemical Plant with Sufficient Separation Margin

Because equivalent inertia is related to speed ratio squared, a high-speed centrifugal compressor with a speed increasing gearbox could also behave similarly to a VFD motor / fan system. A steady-state torsional analysis was performed in the design stage. Results showed that the TNFs should be sufficiently away from the exciting frequencies with the exception of an unavoidable 2nd mode near 50 Hz electrical line frequency. The only possible tuning of this mode was to decrease the high-speed coupling stiffness, but this would result in unacceptable coupling ratings. A stress analysis indicated that the 2nd mode should be acceptable.   During operation, the plant experienced three coupling failures, but these occurred on the low-speed coupling between the motor and gear in the compressor train, which was not considered to be at risk:

- First failure after 121 days operation.
- Second failure after 319 days operation.
- Third failure after 207 days operation.

During the first event, the compressor unit tripped on high vibration due to a failure of the low speed coupling.   A picture of the failed diaphragm coupling is shown in Figure 24.   The coupling manufacturer concluded that the failure was due to torsional fatigue (Corcoran, et al., 2010). Furthermore, the manufacturer confirmed that the coupling was properly sized for this application, speed, and load.   Metallurgical study

indicated fatigue cracks.   All of these coupling failures exhibited characteristics typical of high torsional vibration.
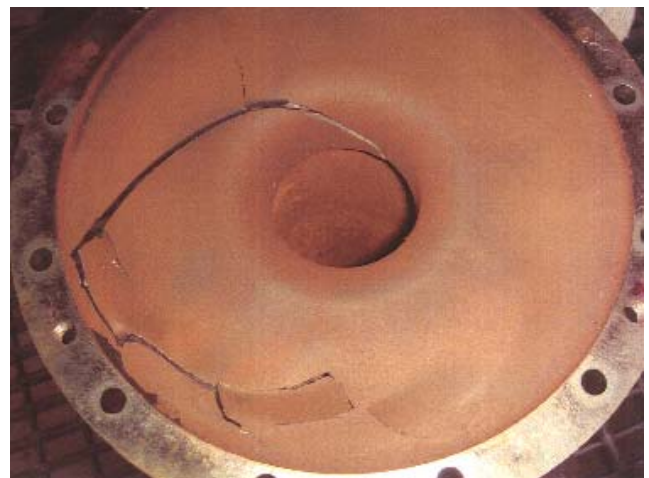

Figure 24. Failed Diaphragm Coupling.

In general, induction motors, gearboxes, and centrifugal compressors do not normally produce significant torsional excitation.   For these types of rotating systems, the transmitted torque should be smooth (less than 10% dynamic torque); however, as noted in several reference papers, VFDs have been shown to create significant torsional excitation in systems and caused torsional vibration and failures of the system.

Various tests were performed by sweeping the speed of the VFD motor.   The first TNF was measured at 13.5 Hz.   This

compared to the predicted TNF of 12 Hz or 720 CPM; therefore, the actual first TNF was 12.5% higher than predicted. One area of the mass-elastic model that could be improved was the motor core. The motor should be modeled using multiple inertia and stiffness values instead of a single lump.

Some load was applied to the compressor, but since the plant was not in operation, a true full-load evaluation was not possible. It was found that the first TNF was continually excited by the VFD when in Direct Torque Control Mode as shown in Figure 25. Based on the modeshapes, it is believed that the first TNF and not the second TNF was responsible for the coupling failures.
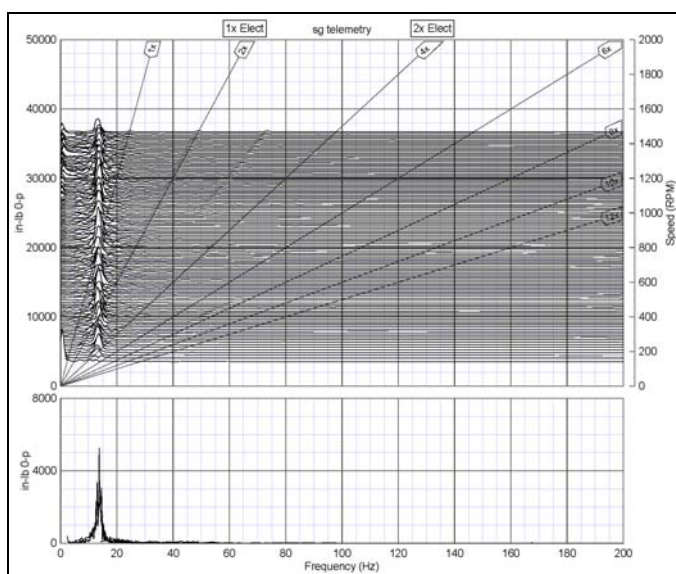
Figure 25. Waterfall Plot of Dynamic Torque During Speed Sweep.

The action of the drive control system is to continuously adjust the power to precisely maintain the speed of the motor. These adjustments can excite the first TNF and put high stresses on the low speed coupling. It was shown that the control system was very sensitive to the time delay parameter. When the time constant was changed to 50 milliseconds, the dynamic torque increased dramatically, although the system was operating well away from the first TNF.

When switched to the basic control method of Scalar Mode without any virtual feedback loops, the excitation was greatly reduced as shown in Figure 26. Note that nothing in the mechanical system was changed, only the operating mode of the VFD was switched.
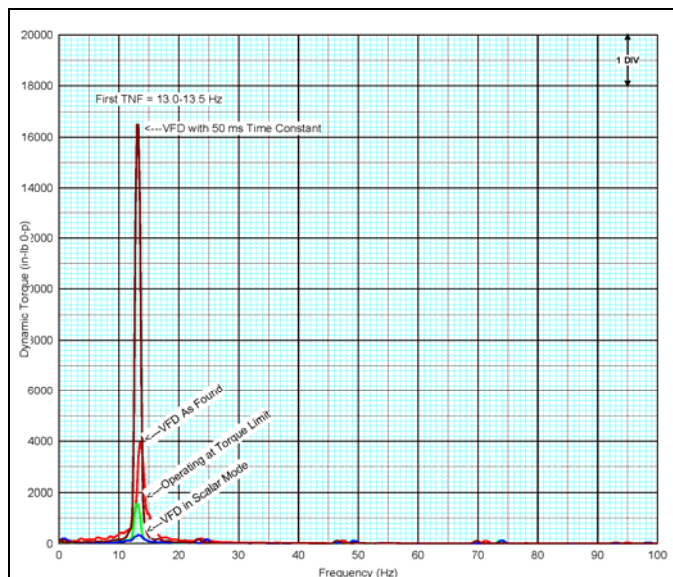

Figure 26. Comparison of Various VFD Operating Modes.

The motor speed is not accurately controlled in the Scalar Mode, but this was not required for the process. Scalar Mode is used in the factory to test motors, but could not be used in the field because of loss of protections. During one test run, it was found that the current spiked, and the motor had to be tripped. It was later concluded that the VFD may have run out of voltage indicating a possible problem with the line power supply at the plant.

One parameter in the VFD control system, Torque Limit, was found to suppress the power fluctuations when activated. When the Torque Limit was reached, the torque fluctuation was reduced. It was later found that the torque limiter is contained in the speed control loop. Therefore, as a short-term solution, the Torque Limit was manually lowered just above the plant operating conditions. With this modification to the VFD controls, the unit has been operating for nearly two years without another coupling failure.

In conclusion, it is believed that many of these VFD torsional problems could be avoided by using a less sophisticated control scheme that would allow for a small amount of speed variation. Precise speed control from the VFD is unnecessary for fans and compressors in most plants. Also, sufficient time for fine tuning the VFD should be allocated during commissioning.

DISCUSSIONS AND CONCLUSIONS

This tutorial has examined torsional prediction accuracy and presented the following:

- Torsional natural frequency error, comparing measured and predicted TNFs for numerous cases.
- Torsional natural frequency repeatability, comparing measured and predicted TNFs for multiple strings of the same design.
- Major sources of uncertainty in torsional modeling.
- Sensitivity to variation in mass-elastic data.
- Methods for conducting torsional tests.

Multiple torsional systems were examined in detail with regard to torsional natural frequency error. For the first natural frequency, the standard deviation between the measured and predicted TNFs of the compressor strings discussed in cases 1 through 13 was approximately 5.5% with worst case errors of -12% and +7%. This is outside of the assumed +/-5% error previously cited by Mondy and Mirro (1982), and assumed by many rotordynamicists.

Uncertainty in coupling stiffness was shown to be a primary contributor to the TNF error. Other contributors to uncertainty include the following:
- Coupling Model
- Stepped Shaft Model
- Motor Core Model
- Gear Mesh Model
- Crankshaft Model
- Proper Consideration of the 1/3 Penetration Rule

Two torsional system designs were examined for repeatability. The first system had a design comprised of a motor and reciprocating compressor. Measurements were made on six strings of equipment. The standard deviation of the first TNF was 1%. A second system had a design comprised of an engine, gearbox, and centrifugal compressor. Measurements were made on seven strings of equipment. The standard deviation of the first TNF was 1.8% for these strings. The variation of TNF for "identical" units is therefore expected to be 1% to 2%.

Results indicate that TNF prediction accuracy better than ±5% should not be assumed. In addition, the results would indicate that TNF error in excess of 5% is not particularly uncommon. This would suggest that either separation margins higher than 10%, or uncertainty modeling of components should be considered when performing the torsional analysis.

At a minimum, these results indicate that the API specification for separation margin could use some clarification with regard to its intent for torsional prediction and measurement. Many rotordynamicists assume the intent is 10% predicted separation margin with an uncertainty of ±5%. Many engineering procurement contractors, on the other hand, believe the intent is 10% actual separation margin including coupling reselection and remanufacture if the margin is not met.

This difference in opinion of how API should be interpreted causes particular difficulties for strings with wide operating speed ranges having numerous potential excitations, many of which may not be of real concern. The safety and reliability of a torsional system is determined by stress, not merely by separation margin from excitation sources that may or may not be of any importance.

API allows the SM requirement to be waived if torsional vibration response is shown to not damage the system when running at resonance. For example, one of the cases described wherein the predicted SM of 11% passed API, but the measured SM of 6% was interpreted to be a violation. The stress analysis indicated that the system was acceptable. For another example, the results of a torsional analysis may show that SM is not required for a modern VFD with low torque ripple (1% or less). This would therefore allow continuous operation over a wide speed range without skip frequencies.

In contrast with SM requirements, recent torsional failures involving VFDs that have been documented in the literature each had sufficient separation margin from running speeds and electrical harmonic frequencies, but still failed due to high non-synchronous excitation from the VFD. A case was presented where extremely high torsional vibration occurred due to instability when operating more than 20% to 30% above the first TNF. Such instability issues with VFD motors seem to occur more often in high inertia systems (i.e. fans) with diaphragm or disc pack couplings that have very low damping.

Such results indicate that a torsional test is valuable not only for verification of separation margin, but also verification of low stress amplitudes and low levels of excitation. In certain cases, verification of separation margins could be considered of secondary importance and validation of the amplitudes the primary factor in determining acceptance. Additional benefits of torsional testing can include assistance with proper tuning of the drive during commissioning along with failure prevention and troubleshooting.

Torsional analytical accuracy is only as good as the accuracy of the data, the programs, and procedures available. The design of reliable systems on the other hand is also dependent on design standards. The API standard requirements provide conservatism in most cases due to the 10% analytical SM requirement as evidenced by the overall lack of torsional failures in API machinery strings where SM from running speed was determined to be the root cause.

In those cases where additional conservatism is required, further system verification can be performed in the form of parametric analysis (considering the errors and uncertainties identified within this paper), stress analysis, torsional measurement, or combination thereof.

NOMENCLATURE

AF	= Amplification Factor
AGMA	= American Gear Manufacturers Association
API	= American Petroleum Institute
CPM	= Cycles Per Minute
FEA	= Finite Element Analysis
G	= System Gain
GD^2	= Mass Moment of Inertia Based on Diameter
Hz	= Hertz (Cycles Per Second)
ID	= Induced Draft (Fan)
J	= Lumped Inertia
K	= Torsional Stiffness
MVR	= Mechanical Vapor Recompression (Fan)
N_c	= Torsional critical speed.
N_1	= Initial (lesser) speed at 0.707 peak amplitude of critical speed.
N_2	= Final (greater) speed at 0.707 peak amplitude of critical speed.
PWM	= Pulse Width Modulation
RPM	= Revolutions Per Minute
SM	= Separation Margin
TNF	= Torsional Natural Frequency
VFD	= Variable Frequency Drive
WR^2	= Mass Moment of Inertia Based on Radius
δ	= logarithmic decrement
ω	= frequency in rad/sec
ζ	= damping ratio
$2\times, 3\times, \ldots$	= harmonics or multiples of fundamental frequency

APPENDIX – TORSIONAL MEASUREMENTS

Various methods of torsional measurement are covered in this appendix. The simplest way some technicians have identified torsional vibration is with a strobe light. For example, "slapping" or "pop canning" of the shim packs in a coupling may be evident when experiencing high torsional vibration. More sophisticated instruments are as follow.

Strain Gage Telemetry System

A strain gage telemetry system can be used to directly measure transmitted and dynamic torque in a shaft or coupling spool piece. The full bridge arrangement with four gages shown in Figure A.1 can measure torsional strain while minimizing the effects of bending strain, axial strain, and temperature changes. The voltage signal produced by the bridge is proportional to strain, but can also be calibrated to output units of shear stress or torque. The measured values can then be compared to allowable limits.
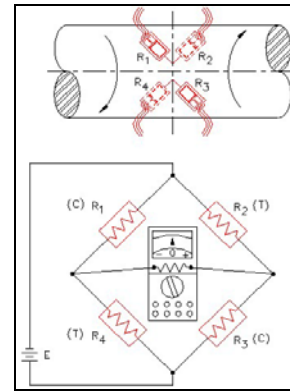

Figure A.1. Full Bridge Arrangement with 4-gages.

Since the strain gages are mounted directly on the rotating shaft, it is necessary to use a wireless telemetry system to transfer the measured strain signals to the recording equipment. Various systems are commercially available. Some require batteries while others use induced power via a radio frequency signal that is inductively coupled from the receiving to the transmitting antenna. The resulting signal is digitized and the digital data stream is reconstructed into an analog signal at the receiver. Although resolution and frequency ranges may vary, typical telemetry systems can have 16-bit resolution and a 0-500 Hz frequency range. Custom systems can have frequency ranges up to 10,000 Hz.

The strain gages should preferably be located where maximum twist occurs, which requires advance knowledge of the torsional mode shapes of the system. Depending on the particular mode shape, the optimum installation location may not be feasible. Installing the gages on the shaft near the coupling hub (but away from any keyways) is usually adequate, or directly on the coupling spool piece if the dimensions are known for the inside / outside diameters and the material shear modulus (Figure A.2). Close-up view of the chevron type strain gage is shown in Figure A.3. Installation of the gages and telemetry system requires several hours with the unit down.

Figure A.2. Strain Gage Telemetry System Installed on Coupling Spool Piece.

Figure A.3. Close-up View of Chevron Style Strain Gage.
Calibration of Strain Gage System

Shunt calibration is usually satisfactory for calibration of the strain gage system. For this method, it is assumed that the strain gages have been properly affixed to the shaft surface and orientated. If so, it is generally thought that the shunt calibration will be within 3% of the actual value, which is more than adequate for most trouble-shooting field studies.

By applying a known unbalance in the bridge circuit, the telemetry system can be calibrated with the shunt resistor. With some telemetry systems, the shunt resistor may be built-in. While at rest, the zero and span can be adjusted on the receiver to obtain a scale factor. Note that the shunt calibration does not take into account possible deviation from the ideal strain/torque relationship due to variation in gage factors and exact gage placement. The shaft diameter should always be verified.

Normally, using a shunt calibration will result in amplitudes within 3% of actual values. If more accuracy is required, such as for measuring efficiency, then a level arm calibration may be needed (see examples in Feese and Hill, 2009). Therefore, a second mechanical calibration could be performed where a known moment was applied directly to the shaft; however, for accurately measuring performance or efficiency, a mechanical calibration test may be necessary using a lever arm arrangement. This requires additional time and advanced planning.

Rotary Shaft Encoder / Gear Teeth / Printed Bar Pattern

A series of pulses can be used to measure the angular position of a shaft. These pulses could be generated by a rotary encoder, gear teeth, or a printed bar pattern depending on the layout of the machinery to be tested.

Rotary encoders are probably the most accurate device for this type of measurement and are normally attached to the free-end of a rotating shaft using an adaptor as shown in Figure A.4. Setup and use of the encoder is typically simple and straightforward; however, the shaft must have proper accommodations for the encoder, such as a tapped hole in the shaft end.
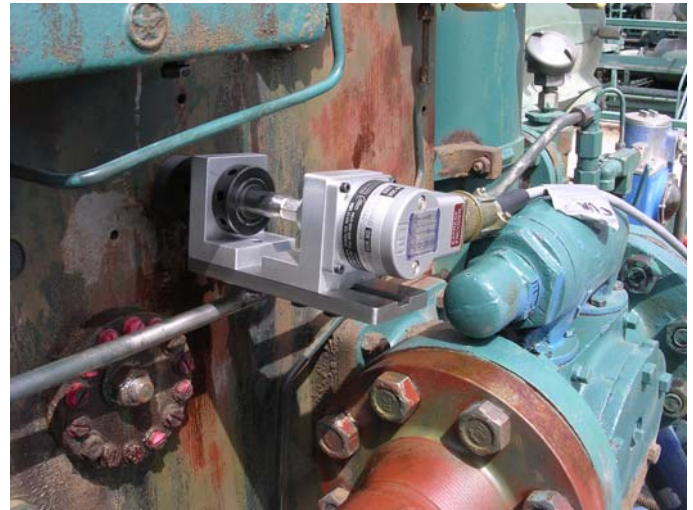

Figure A.4. Encoder on End of Compressor Crankshaft.

An alternate way to install an encoder is shown in Figure A.5. In this case, a jack shaft from the front of the engine was driving a cooling fan, which prevented installing the encoder directly to the engine crankshaft; therefore, a special mounting bracket was designed with a spring to apply a constant force to the encoder wheel to prevent slippage relative to the jack shaft. The measurements were adjusted by the diameter ratio of the jack shaft and the rider wheel.
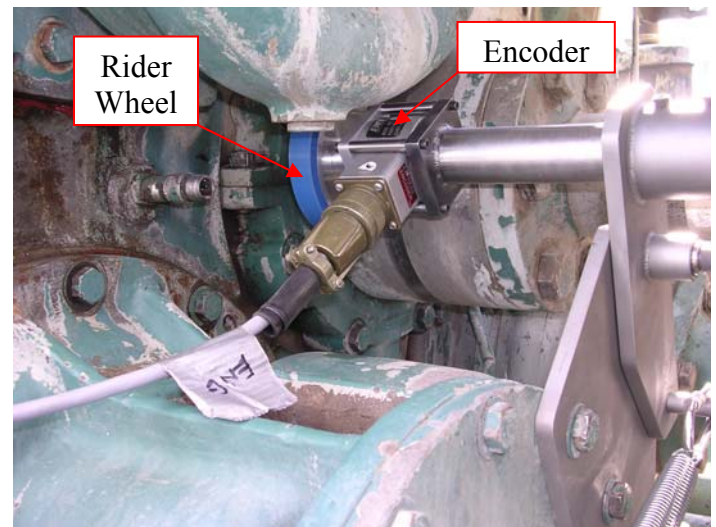

Figure A.5. Encoder with Rider Wheel.

Similar to shaft encoders, the frequency modulation system uses proximity probes or magnetic pick-ups to measure the pulse rate or gear tooth passing frequency (Figure A.6). Assuming the gear teeth are equally spaced and the lateral vibration is low, variations in time between tooth-passing will indicate torsional vibration. The signal can be demodulated and converted to angular velocity or integrated to angular displacement. Lateral vibration or non-uniform profile could affect results. Two probes, 180 degrees apart, are preferred to cancel the effects of lateral vibration.
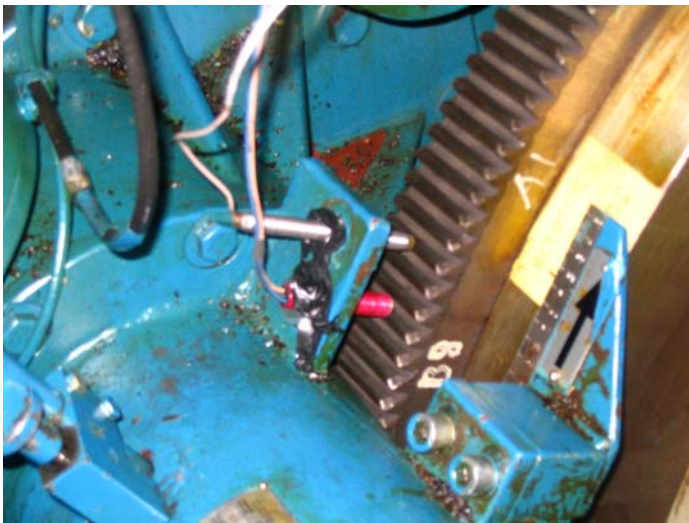
Figure A.6. Proximity Probe Pick-up on Engine Flywheel.

Figure A.8. Comparison of Processing Techniques.

Printed bar patterns can also be used as shown in Figure A.7. However, it is important that the spacing of the pattern be even. Overlap at the ends can cause a problem. Also, the optical device used to trigger the pulses must be able to react quickly enough. Not all optical tachometers have high enough frequency response for this application.
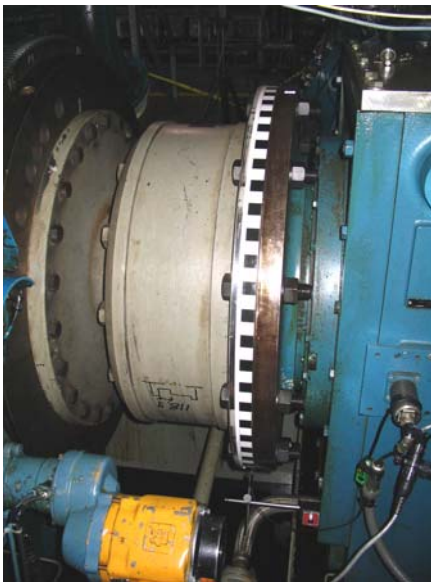

Figure A.7. Printed Black/White Pattern on Coupling Flange.

Regardless of the method used to generate the pulses, additional processing is needed to determine rotational speed and torsional vibration. There are several hardware options available. These perform satisfactorily for steady-state conditions, but may create low-frequency noise (ski-slope) during speed changes due to analog integrators. Software utilizing the Hilbert transform can also be used to measure torsional vibration (Randall, 1990). The Hilbert transform does not require as high of sampling rate and produces good waterfall plots during speed ramps. This technique can also be used with two pulse signals and a known torsional stiffness to measure torque. A comparison between hardware and software options is shown in Figure A.8 using real test data.
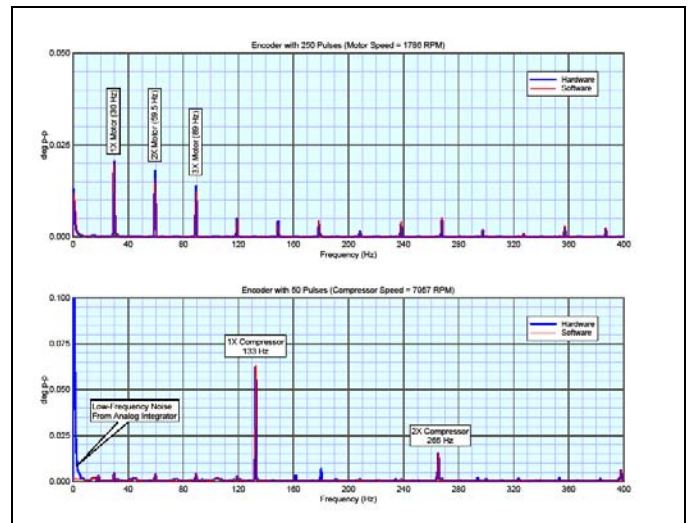
Laser Vibrometer

A laser vibrometer can be used to measure angular displacement in degrees. The laser is non-contacting and can be "pointed" at the rotating surface of interest. No downtime is normally required for installation; however, the laser vibrometer may not be capable of accurately evaluating transient conditions, such as start-ups, speed sweeps, or shutdowns. This could limit its ability to measure natural frequencies of a system if speed changes occur too quickly. Newer laser vibrometers have a frequency range down to 0.5 Hz and a dynamic range of 0.01 to 12 degrees.

Laser vibrometer are sometime mounted on a flexible stand or deck. Excessive vibration of the laser head could affect torsional vibration readings. Likewise, vibration of the torsiograph or non-centered application could cause erroneous readings. Figure A.9 shows a typical laser setup.

Figure A.9. Laser Aimed at Reflective Tape on Jack Shaft.

Example of Laser Measurement on Engine

A Polytec laser was used to measure torsional vibration on the front end of a gas engine (Feese and Smith, 2009). As shown in Figure A.9, two red dots can be seen from the laser beams on the reflective tape wrapped around the jack shaft. The laser is powered by a separate computer module, which processes the signal, applies filters, and produces a voltage proportional to torsional oscillation in degrees.

Torsiograph

A torsiograph is an instrument that rotates with the shaft and is used to measure angular velocity (deg/sec) or displacement (degrees). For example, an HBM torsiograph operates on the seismometer principle, with a mass retained by springs whose relative motion compared to the stator is converted into an electrical signal by inductive proximity detectors (Figure A.10). The frequency range is approximately 3 - 1,000 Hz. At the lower frequency range, the internal masses and springs have a resonance near 3 Hz.

Figure A.10. Torsiograph on Oil Pump End of Compressor.

The device must be mounted on a free end of the shaft, preferably near an anti-node or point of maximum torsional oscillation for best results. While the instrument is easy to install once an adaptor has been fabricated, it is sensitive to lateral vibration and will require that the shaft end be true and drilled and tapped such that the torsiograph is centered on the shaft. Downtime of the compressor system will be required for installation.

The amount of oscillation may not be an indicator of shaft stresses. For example, high oscillation can occur in a system with a soft coupling, but the stresses may be low. If only torsional oscillations are measured, the torsional analysis should be normalized based on the measurements to evaluate the stresses in the system. Torsiographs have been used to evaluate oil pumps on reciprocating compressors and fan blade failures on a gearbox. The gear pump would be removed and an electric oil pump temporarily used for the test.

Unfortunately, HBM torsiographs are no longer manufactured. Some specifications, particularly from water districts and municipalities, may still call for a "torsiograph test"; however, today shaft encoders and torsional lasers are more commonly used to measure torsional vibration instead of a torsiograph.

Inductive Torque Measurement

A new method for measuring torque is a contactless inductive sensor that measures the magnetic permeability variation of a shaft material (Figure A.11). The concept is based on the anisotropic magnetostrictive effect in ferromagnetic shaft surfaces (Fraunhofer, 2007). The magnetic permeability of the shaft material differs in the tensile versus compressive directions and is proportional to the torsional stress. The sensor is able to measure the permeability variation at the surface over a wide torque range. The sensor requires a narrow air gap (similar to a proximity probe), and typically has a frequency range of 0 – 200 Hz.
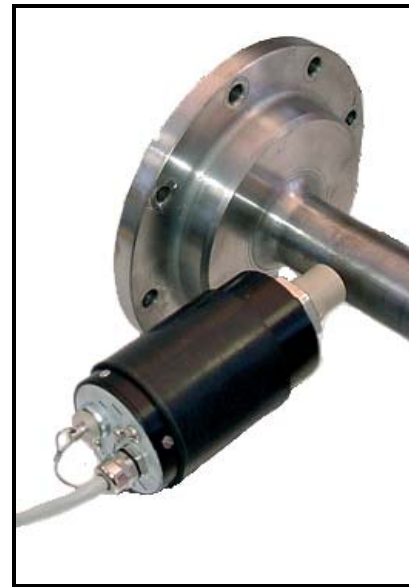

Figure A.11. Inductive Torque Measurement.

Inferring Torque from Vibration of Gears

Recall that torsional vibration is normally silent except for a gearbox. Therefore, it may be possible to infer torque from vibration measurements on a gearbox. On a recent job involving a VFD motor – gearbox – centrifugal compressor, strain gage measurements were made near the low speed coupling as well as shaft vibration readings from proximity probes for the LS gear and HS pinion shafts.

The most significant dynamic torque occurred at the first TNF of 13 Hz. Transfer functions were calculated for each probe. It was found that the best probes were in the Y direction for the LS gear and in the X direction for the HS pinion. At the frequency of interest, the coefficients were approximately 185,000 to 230,000 in-lb of torque per mil of lateral shaft vibration. For example, 0.185 mils p-p of lateral shaft vibration indicated 34,000 in-lb p-p of dynamic torque at 13 Hz. Note that the transfer functions would be different for other frequencies and other gearboxes.

This approach could be used for simple long-term monitoring when a torsional device is difficult to install. For example, the proposed method was sensitive enough to detect sidebands with 13 Hz spacing in the HS pinion vibration readings when the dynamic torque reached a high level. Estimation of shaft torque from shaft vibration was also discussed by Tanaka, et al., (2009).

Electrical Measurements

It may be necessary to measure voltage and current to help diagnose the torsional vibration problems with systems involving electric motors. For example, VFDs can produce torque ripple at multiples of electrical frequency, which can excite torsional natural frequencies of the system (Feese and Maxfield, 2008). Electrical measurements can be used to determine electrical power and the amount of torque fluctuation potentially being applied to the motor by the drive. Another example is when reciprocating compressors cause current pulsation in motors that experience high torsional oscillation. The National Electrical Manufacturers Association (NEMA 2011) specification states that current pulsations should not exceed 66% in order to prevent flickering of lights and other electrical problems.

The stator voltages can be measured with voltage dividers, which have a large frequency response well in excess of 10,000 Hz. Figure A.12 shows three stator voltage probes (one for each phase) inside a motor cabinet. The output signal from the voltage probes requires impedance matching (1 MW) and in some cases amplification.
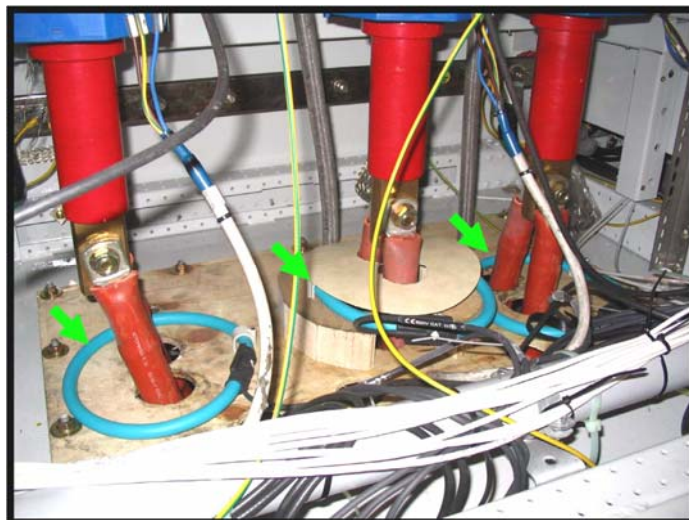

Figure A.13. Current Probes.

Figure A.12. Voltage Probes.

Stator currents can be measured using a flexible head that mounts around the phase cables. The current probes are based on the Rogowski principle. Figure A.13 shows the installation of the stator current probes around each of the three phases in the motor junction box. If DC current values are needed, then a Hall Effect transducer must be used.

REFERENCES

AGMA 9004, "Flexible Couplings – Mass Elastic Properties and Other Characteristics," December 2008.

Alexander, K., Donohue, B., Feese, T., Vanderlinden, G., Kral, M., "Failure Analysis of MVR (Mechanical Vapor Recompressor) Impeller," *Engineering Failure Analysis*, Volume 17, Issue 6, Elsevier, September 2010.

API Standard 617, 1973, "Centrifugal Compressors for General Refinery Services," Third Edition, American Petroleum Institute, Washington, D.C.

API Standard 617, 2002, "Axial and Centrifugal Compressor and Expander-Compressors for Petroleum, Chemical, and Gas Refinery Services," Seventh Edition, American Petroleum Institute, Washington, D.C.

API Standard 671, "Special Purpose Couplings for Petroleum, Chemical and Gas Industry Services," September 2010.

API Standard 684, "API Standard Paragraphs Rotordynamic Tutorial: Lateral Critical Speeds, Unbalance Response, Stability, Train Torsionals, and Rotor Balancing," 2nd Edition, August 2005.

Bosin, D., Ehrich, R., and Stark, M., 1999, "Torsional Instabilities of Motor Driven Turbomachinery," *Turbomachinery International*, pp 18-20.

Calistrat, M. M., and Leaseburge, G. G., 1972, "Torsional Stiffness of Interference Fit Connections," ASME Paper 72-PTG-37.

Corcoran, Kocur, and Mitsingas, "Preventing Undetected Train Torsional Oscillations," *Proceedings of the 39th Turbomachinery Symposium*, Houston, Texas 2010.

Dawson, B. and Davies, M., 1975, "An Improved Holzer Procedure for Torsional Vibration Analysis," *The Journal of Mechanical Engineering Science*, 17, 1, pp 26-30.

De Choudhury, P., "Torsional Analysis of Unit 59-K-400A – Comparative Study with Comments," Elliott Company Inter-Office Letter, April 3, 1979.

Ewins, D.J., 2000, *Modal Testing: Theroy, Practice and Application, Second Edition*, Research Studies Press Ltd.

Feese, T.D., and Hill, C.H., 2009, "Preventing Torsional Vibration Problems in Reciprocating Machinery," *Proceedings of the Thirty-Eighth Turbomachinery Symposium*, Turbomachinery Laboratory, Texas A&M University, College Station, Texas, pp. 213-238.

Feese, T.D. and Maxfield, R., 2008, "Torsional Vibration Problem with Motor/ID Fan System Due to PWM Variable Frequency Drive," *Proceedings of the Thirty-Seventh Turbomachinery Symposium*, Turbomachinery Laboratory, Texas A&M University, College Station, Texas, pp 45 – 56.

Feese, T.D. and Smith, D.R., 2009, "Critical Equipment Measured in the Field," Polytec InFocus, Issue 01.

Fraunhofer ITWM, "A Contactless Torque Sensor for Online Monitoring of Torsional Oscillations," 2007.

Holset Flexible Couplings Catalog, 510/3.90/F.H., *Application Information Type PM – Industrial*, Cincinnati, Ohio.

Hudson, J., Feese, T., "Torsional Vibration – A Segment of API 684," *Proceedings of the 35th Turbomachinery Symposium*, Texas A&M University, College Station, Texas, 2006.

Ker Wilson, W., *Practical Solution of Torsional Vibration Problems, Volume 1,* New York, New York: John Wiley and Sons, 3rd Ed., 1956.

Kerkman, R.J., Theisen, J. and Shah, Kirti, 2008, "PWM Inverters Producing Torsional Components in AC Motors," *Petroleum and Chemical Industry Technical Conference*, PCIC 2008. 55th IEEE.

Kocur, J.A. and Muench, M.G., "Impact of Electrical Noise on the Torsional Response of VFD Compressor Trains," *Proceedings of the First Middle East Turbomachinery Symposium*, 2011.

Meirovitch, L., 1986, *Elements of Vibration Analysis*, New York, New York: McGraw-Hill Inc.

Mondy, R. E. and Mirro, J., 1982, "The Calculation and Verification of Torsional Natural Frequencies for Turbomachinery Equipment Strings," Proceedings of the Twelfth Turbomachinery Symposium, Turbomachinery Laboratory, Texas A&M University, College Station, Texas, pp. 151-156.

Murray, B.D., Howes, B.C., Zacharias, V., Chui, J., "Sensitivity of Torsional Analyses to Uncertainty in System Mass-Elastic Properties," Presented at the International Pipeline Conference, Calgary, Alberta, June 1996.

NEMA Standards Publication MG 1-2011, *Motors and Generators*, Rosslyn, Virginia, 2011.

Nestorides, E.J., *A Handbook on Torsional Vibration*, Cambridge, 1958.

Pettinato, B. C., Kocur, J. A., and Swanson, E., 2011, "Evolution and Trend of API 617 Compressor Rotordynamic Criteria," Turbomachinery Society of Japan, 39, 5, pp 36-47.

Piergiovanni, L. S., Lerch, E., Zurowski, R., Kumar, S. B., Osman, R., Deo, B., Bahr, B., Sakaguchi, J., Okazaki, Y., and Saito, T., 2010, "Investigation of Subsynchronous Torsional Interaction on LNG Power Plants," *Proceedings of the 16th International Conference & Exhibition on Liquefied Natrual Gas*, Oran, Algeria.

Pollard, E. I., 1967, "Torsional Response of Systems," ASME Journal of Engineering for Power, 89, 3, pp 316-324.

Pollard, E. I., "Torsional Critical Speed Test Report: Turbine Driven Centrifugal Compressors," Elliott Company Inter-Office Letter, June 15, 1972.

Randall, R.B., "Hilbert Transform Techniques for Torsional Vibration," The Institution of Engineers Australia Vibration and Noise Conference, 1990.

Steiner, S., 2007, "Revisiting Torsional Stiffness," Gas Machinery Research Council Conference, Dallas, TX.

Sohre, J.C., 1965, "Transient Torsional Criticals of Synchronous Motor-Driven, High-Speed Compressor Units," ASME Paper No. 65-FE-22.

Tanaka, Adachi, Takahashi, and Fukushima, "Torsional-Lateral Coupled Vibration of Centrifugal Compressor System at Interharmonic Frequencies Related to Control Loop Frequencies in Voltage Source Inverter," Proceedings of 38th Turbomachinery Symposium, Case Study,

Vance, J. M., Murphy, B. T., and Tripp, H. A., 1984, "Critical Speeds of Turbomachinery: Computer Predictions vs Experimental Measurements," Proceedings of the Thirteenth Turbomachinery Symposium, Turbomachinery Laboratory, Texas A&M University, College Station, Texas, pp. 105-130.

Wachel, J. C. and Szenasi, F. R., 1993, "Analysis of Torsional Vibrations in Rotating Machinery," *Proceedings of the Thirteenth Turbomachinery Symposium*, Turbomachinery Laboratory, Texas A&M University, College Station, Texas, pp. 127-151.

ACKNOWLEDGMENTS